ISSN 0003-0007

Volume 77
Number 1
January 1996

bulletin of the American Meteorological Society

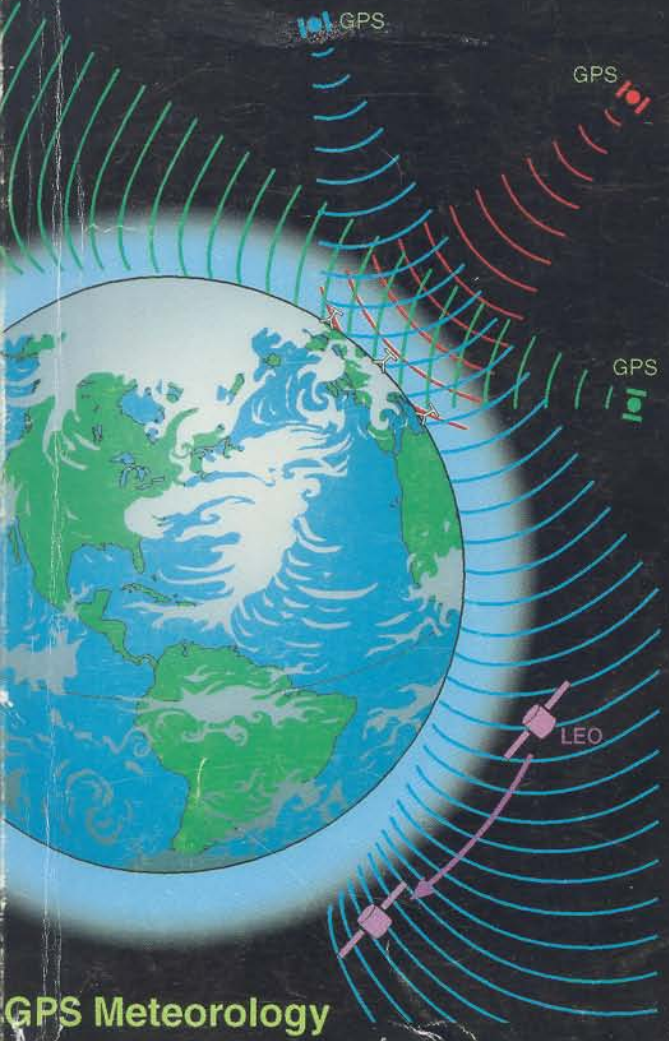

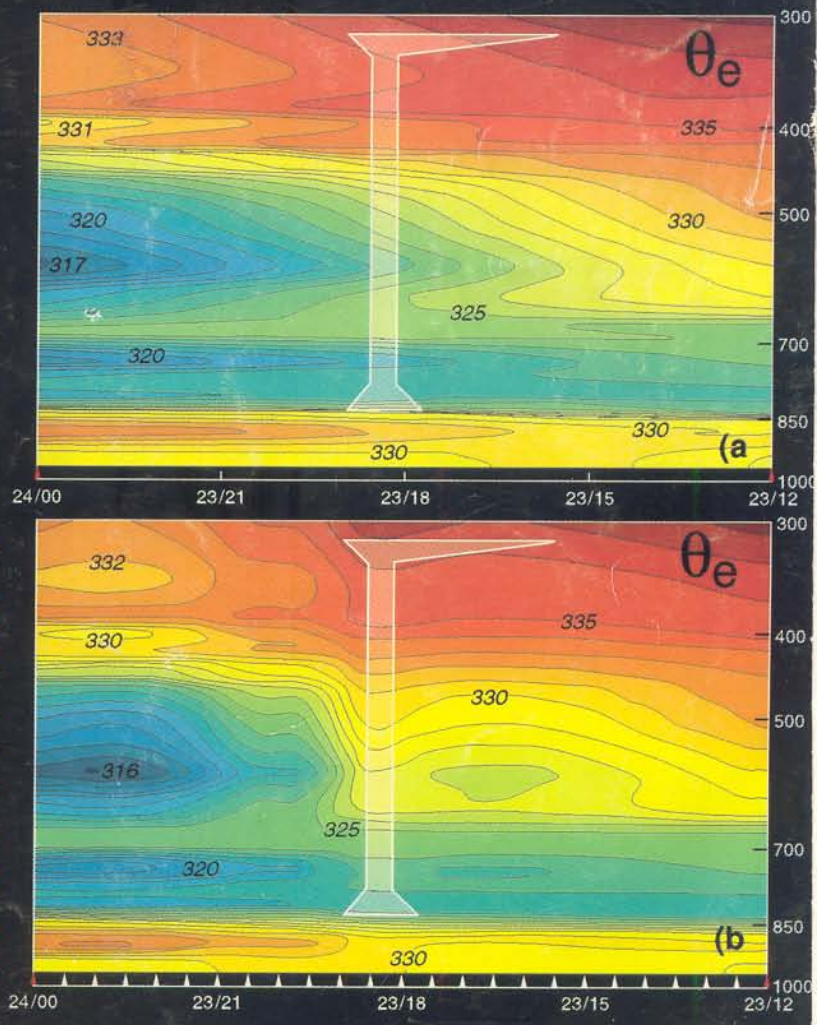

GPS Meteorology

GPS Sounding of the Atmosphere from Low Earth Orbit: Preliminary Results

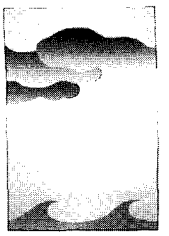

R. Ware,* M. Exner,+ D. Feng,# M. Gorbunov,@ K. Hardy,& B. Herman,# Y. Kuo,**
T. Meehan,++ W. Melbourne,++ C. Rocken,* W. Schreiner,+ S. Sokolovskiy,@
F. Solheim,* X. Zou,** R. Anthes,+ S. Businger,## and K. Trenberth**

ABSTRACT

This paper provides an overview of the methodology of and describes preliminary results from an experiment called GPS/MET (Global Positioning System/Meteorology), in which temperature soundings are obtained from a low Earth-orbiting satellite using the radio occultation technique. Launched into a circular orbit of about 750-km altitude and 70° inclination on 3 April 1995, a small research satellite, *MicroLab 1,* carried a laptop-sized radio receiver. Each time this receiver rises and sets relative to the 24 operational GPS satellites, the GPS radio waves transect successive layers of the atmosphere and are bent (refracted) by the atmosphere before they reach the receiver, causing a delay in the dual-frequency carrier phase observations sensed by the receiver. During this occultation, *GPS limb sounding* measurements are obtained from which vertical profiles of atmospheric refractivity can be computed. The refractivity is a function of pressure, temperature, and water vapor and thus provides information on these variables that has the potential to be useful in weather prediction and weather and climate research.

Because of the dependence of refractivity on both temperature and water vapor, it is generally impossible to compute both variables from a refractivity sounding. However, if either temperature or water vapor is known from independent measurements or from model predictions, the other variable may be calculated. In portions of the atmosphere where moisture effects are negligible (typically above 5–7 km), temperature may be estimated directly from refractivity.

This paper compares a representative sample of 11 temperature profiles derived from GPS/MET soundings (assuming a dry atmosphere) with nearby radiosonde and high-resolution balloon soundings and the operational gridded analysis of the National Centers for Environmental Prediction (formerly the National Meteorological Center). One GPS/MET profile was obtained at a location where a temperature profile from the Halogen Occultation Experiment was available for comparison. These comparisons show that accurate vertical temperature profiles may be obtained using the GPS limb sounding technique from approximately 40 km to about 5–7 km in altitude where moisture effects are negligible. Temperatures in this region usually agree within 2°C with the independent sources of data. The GPS/MET temperature profiles show vertical resolution of about 1 km and resolve the location and minimum temperature of the tropopause very well. Theoretical temperature accuracy is better than 0.5°C at the tropopause, degrading to about 1°C at 40-km altitude.

Above 40 km and below 5 km, these preliminary temperature retrievals show difficulties. In the upper atmosphere, the errors result from initial temperature and pressure assumptions in this region and initial ionospheric refraction assumptions. In the lower troposphere, the errors appear to be associated with multipath effects caused by large gradients in refractivity primarily due to water vapor distribution.

1. Introduction

On 3 April 1995, a Pegasus rocket carried aloft by an aircraft from Vandenburg Air Force Base launched a small research satellite (*MicroLab 1*) into a circular orbit of about 750-km altitude and 70° inclination. The disk-shaped satellite, which circles Earth every 100 min, carried a laptop-sized Global Positioning System

*University Navstar Consortium, Boulder, Colorado.
+University Corporation for Atmospheric Research, Boulder, Colorado.
#The University of Arizona, Tucson, Arizona.
@Russian Institute of Atmospheric Physics, Moscow, Russia.
&Lockheed Martin Missiles and Space, Palo Alto, California.
**National Center for Atmospheric Research, Boulder, Colorado.
++Jet Propulsion Laboratory, California Institute of Technology, Pasadena, California.
##University of Hawaii at Manoa, Honolulu, Hawaii.
Corresponding author address: Richard A. Anthes, University Corporation for Atmospheric Research, 1850 Table Mesa Dr., Boulder, CO 80303.
In final form 15 September 1995.
©1996 American Meteorological Society

(GPS) receiver to demonstrate sensing of the terrestrial atmosphere by the GPS limb sounding method (Melbourne et al. 1988; Ware 1992). This paper describes the first results from the GPS/Meteorology (GPS/MET) proof-of-concept experiment[1] (Ware et al. 1993).

The Global Positioning System is an advanced satellite navigation system offering precision global services. The system includes a constellation of 24 operational satellites and an extensive ground control system. Although GPS was developed for military needs, numerous scientific and commercial applications have matured in parallel, and the number of new applications is growing rapidly (Bevis et al. 1992; Ware and Businger 1995). It now appears that GPS is destined to become, in effect, a global utility upon which many manufacturing and service industries will rely.

In a companion paper, Businger et al. (1996) provide an overview of the applications of GPS in atmospheric science. They discuss the use of ground-based GPS receivers to estimate precipitable water with an accuracy comparable to, and in some cases better than, that of water vapor radiometers. In the GPS limb sounding method (Fig. 1), atmospheric soundings are retrieved from observations obtained when the radio path between a GPS satellite and a GPS receiver in low Earth orbit (LEO) traverses Earth's atmosphere (Hardy et al. 1992). When the path of the GPS signal begins to transect the mesopause at about 85-km altitude, it is sufficiently retarded that a detectable 1-mm (3×10^{-12} s) delay in the dual-frequency carrier phase is observed by the LEO GPS receiver. GPS transmitter and LEO receiver clock errors are minimized through differencing of LEO GPS data with ground-based GPS data from tracking stations supported by the National Aeronautics and Space Administration (NASA) and the International GPS Service (Zumberge et al. 1994; Ware and Businger 1995). As the signal path descends through successively denser layers of the atmosphere, the excess path increases to approximately 1 km (3×10^{-6} s) at Earth's surface. Thus, the atmosphere creates a signal with about six orders of magnitude in dynamic range.

A single LEO GPS receiver can observe more than 500 occultations per day, with roughly uniform global coverage. This method promises to provide valuable measurements of refractivity. As discussed in the appendix, refractivity depends on temperature and water vapor through two terms, a *dry* and a *wet* term. Without knowing one term or the other, neither temperature nor moisture profiles can be recovered in the general case. Therefore, when temperature profiles are the goal, GPS limb sounding is useful only where moisture effects are negligible (and, hence, temperature can be calculated directly from refractivity with the wet term set to zero), including stratospheric, upper-tropospheric, polar, and other regions of the atmosphere with temperatures lower than 250 K, or where ancillary water vapor or temperature estimates are available (such as from independent measurements, model predictions, or climatology). However, as shown later, refractivity itself may be valuable in weather forecasting and as a global temperature change signal.

2. History of radio occultation methodology

The atmospheric measurements reported here are based on a radio occultation technique that was first developed at the Jet Propulsion Laboratory (JPL) and used by Stanford University for application to studies of planetary atmospheres and ionospheres. Radio occultation experiments at JPL and Stanford have played a prominent role in the NASA program for

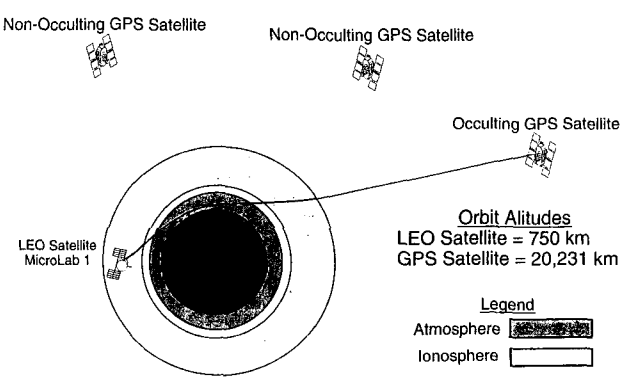

FIG. 1. Schematic of a GPS/MET sounding of the Earth's atmosphere (not to scale). The ray path descent through the neutral atmosphere lasts a minute or more, depending on the relative positions of Earth and the LEO and GPS satellites. Radio path delays observed as the ray path approaches the Earth's surface can be as large as several kilometers with ray path bending as large as 1 deg. Path delay profiles can be converted to refractivity profiles.

[1]The University Corporation for Atmospheric Research (UCAR) has a contract with Orbital Sciences Corporation, operator of *MicroLab 1*, that gives UCAR exclusive rights to the GPS/MET data for scientific use. UCAR is providing the data free of charge to scientists around the world via the World Wide Web (http://pocc.gpsmet.ucar.edu).

solar system exploration for more than three decades. They have contributed uniquely to studies of the atmospheres of Venus (Kliore et al. 1965; Fjeldbo and Eshleman 1969; Fjeldbo et al. 1971; Newman et al. 1984), Mars (Fjeldbo and Eshleman 1968; Lindal et al. 1979), the gas giants Jupiter, Saturn, Uranus, and Neptune (Lindal et al. 1981, 1985, 1987, 1990; Lindal 1992) as well as the outer-planet satellites Io, Titan, and Triton (Kliore et al. 1975; Lindal et al. 1983; Tyler et al. 1989), and to studies of planetary ring structure (Tyler 1987).

Typically, experiments involved a spacecraft transmitter linked to a terrestrial receiver via a centimeter-wavelength radio signal. The spacecraft trajectory was selected so that the propagation path from the spacecraft to Earth passed through the planetary atmosphere under study, producing distinctive variations in the amplitude and phase of the received signal. These variations were then used to infer the thermodynamic structure of the atmosphere of these planets.

Russian scientists investigated the potential of the occultation technique, aided by refraction observations from space, of the Sun as it is occulted by Earth's atmosphere (Gurvich et al. 1982). Subsequently, the use of GPS occultations for sensing the terrestrial atmosphere was proposed by Melbourne et al. (1988). More recently, investigators at JPL conducted experiments designed to refine the occultation methodology for use in sensing Earth's atmosphere, using a high-performance GPS receiver from a mountain top (Meehan et al. 1991). This experience base, combined with the availability of GPS, set the stage for development of an accurate and reliable method for remote sensing of the terrestrial atmosphere.

3. Characteristics of other upper-air observational systems

To put the characteristics of GPS limb sounding data and the preliminary GPS/MET temperature retrievals discussed later (section 7) into perspective, we first summarize the characteristics of other upper-air observational systems.

a. Radiosondes

Since the establishment of the global radiosonde network beginning in the 1940s, radiosondes have been the mainstay of the global upper-air observing system. In 1991 there were more than 1000 radiosonde stations operated by 92 nations using 39 different types of radiosondes (NOAA 1992). Under ideal conditions and careful calibration, radiosondes are quite accurate, with temperatures accurate to about ±0.5°C and relative humidities accurate to within a few percent, except under very low temperatures or very high or low relative humidities (Shea et al. 1994; Ahnert 1991; Luers and Eskridge 1995). Under operational conditions, relative humidity measurement errors are considerably greater than a few percent. Radiosondes provide data from near the surface to a height of about 30 km. Because of pressure errors, temperature accuracies are degraded in the upper troposphere and stratosphere, with typical errors of 1°C above 250 mb increasing to as large as 4°C at 10 mb (Nash and Schmidlin 1987). Radiosondes produce soundings with high vertical resolution, resolving features with vertical scales of a few tens of meters. However, the coverage of radiosondes is uneven over the globe and sparse to nonexistent over the oceans. The temporal resolution is also fairly low (12-h frequency at best, and many countries take only one observation per day), and they suffer from substantial changes in instrumentation with time (e.g., Schwartz and Doswell 1991). In particular, for humidity, complicating factors have been the use of low-quality sensors and changes in the type of humidity sensing element and, more important, changes in reporting procedures at low humidity (e.g., Elliott and Gaffen 1991). Costs are an additional issue, especially for developing countries. The upper-air radiosonde-observing network reached its peak during the Global Weather Experiment (1979), and the number of soundings has since declined by about a third (Trenberth 1995).

b. Satellites

Since the first meteorological satellite, *TIROS-1,* was launched on 1 April 1960, satellites have played an increasingly important role in providing first meteorological images and later temperature, moisture, and wind data for use in operational weather prediction and for research. *TIROS-1* provided only cloud images; the first satellite producing wind data was *ATS-1,* launched 6 December 1966. The first satellite producing temperature and water vapor soundings was *Nimbus III,* launched in 1969. The first operational satellite producing temperature and water vapor soundings was *NOAA-2,* launched in 1972.

Atmospheric soundings are produced by satellites in polar and geostationary orbits. The present generation of operational polar orbiters began with NASA's

prototype *TIROS-N,* launched in 1978, followed in 1979 by *NOAA-6,* the first operational spacecraft in the series, and based on the design of NASA's *TIROS-N.* Two of these satellites usually operate simultaneously, one in a morning and the other in an afternoon orbit around Earth, thus providing four observations of the entire Earth each day. These satellites carry the High Resolution Infrared Sounder, stratospheric sounder unit, microwave sounding unit (MSU), and the Advanced Very High Resolution Radiometer. Data from the microwave radiometers are unaffected by clouds and light rain, but those from the infrared radiometers are contaminated by clouds and aerosols.

The United States operates two Geostationary Operational Environmental Satellites (GOES) located over the equator at about 75° and 135°W longitude. They provide frequent cloud images, from which cloud motions are measured to estimate winds at cloud altitudes, and soundings of a large portion of the Western Hemisphere. The first of a completely new design, *GOES-8,* became operational early in 1995, and the second was successfully launched 23 May 1995. Japan and Europe also operate meteorological satellites in geostationary orbit and make the data available to the world. However, neither satellite includes sounding capabilities.

Vertical profiles of temperature and water vapor are determined from satellites by instruments that detect radiances, or electromagnetic energy emitted at specific wavelengths or frequencies. The instruments are designed to measure radiation in wavelengths or spectral channels that originate in broad layers in the atmosphere. For example, the Visible and Infrared Spin Scan Radiometer (VISSR) Atmospheric Sounder, which has been carried on the GOES since September 1980, is composed of 12 channels. Three of these peak at the surface, and the others peak at 950, 850, 600, 500, 450, 400, 150, 70, and 40 mb (Hayden 1988). The new GOES sounder has 19 channels.

Given a first-guess temperature and moisture profile, the radiative transfer equations can be "inverted" using the observed radiances in these channels to produce temperature and moisture profiles. The inversion process involves calculating temperature and moisture corrections to the first guess based on differences between the observed and calculated radiances or "brightness temperatures."

It is difficult to estimate the accuracies and other characteristics of such satellite-derived soundings because they are highly dependent on the quality of the first-guess profiles. However, some general statements may be made. Sources of error include contamination by clouds and aerosols (with infrared sounders), space–time sampling problems, instrumentation limitations, and calibration drift. Because the satellites detect vertically integrated radiances, the vertical resolution is generally rather coarse (typically greater than 5 km), and atmospheric temperature inversions, including the tropopause, are often missed or smoothed heavily. The low vertical resolution also tends to introduce biases in the soundings. Horizontal gradients of temperature and moisture tend to be underestimated by the retrievals due to the poor vertical resolution of passive sounders. Hayden (1988) gives a table of statistics of satellite retrievals of temperature and dewpoint compared to the best estimate of these values over a data-rich region. From this table, we estimate typical errors of satellite retrievals of temperature and dewpoint to be in the range of 1°–2°C and 4°–10°C, respectively. This estimate is consistent with the results of a comparison of layer mean temperatures derived from radiosondes and satellites by Lee and Schmidlin (1991), who found that the satellite-retrieved layer temperature agreed with the radiosonde within ±1.2°C. High spectral resolution infrared instruments containing several thousand spectral channels are under development and have the potential to improve the vertical resolution and accuracy of satellite nadir soundings (Smith et al. 1990).

Global atmospheric temperature datasets have been constructed from satellite MSU measurements of the National Oceanic and Atmospheric Administration's (NOAA) polar satellite series (Spencer and Christy 1990; Spencer et al. 1990). MSUs sample the entire globe twice daily from each of the two satellites with different equator-crossing times. One MSU channel is sensitive to thermal emission from molecular oxygen in the middle troposphere and is relatively insensitive to water vapor and the Earth's surface, thereby providing excellent long-term stability required for atmospheric monitoring. Moreover, the excellent agreement between two MSUs on different satellites (*NOAA-6* and *NOAA-7*), where the monthly mean hemispheric temperatures are reproduced to within about 0.01°C, confirms the suitability of this channel as a monitoring tool. The temperature-weighting function for channel 2 has a broad peak near 500 mb. Trenberth et al. (1992) and Hurrell and Trenberth (1992) have evaluated the MSU observations and compared them with surface and numerical weather model temperatures throughout the atmosphere. They

conclude that MSU temperatures are a valuable tool for monitoring global temperatures. However, MSU observations are limited because they lack vertical resolution and cannot resolve critical structures like the tropopause and other temperature inversions.

Satellite soundings of atmospheric moisture from Special Sensing Microwave/Imager microwave measurements from the polar-orbiting Defense Meteorological Satellite Program spacecraft (Schlussel and Emery 1990) are useful for the total-column integral (the precipitable water). However, these and infrared sounders are unable to provide useful information on the vertical profiles and structure of moisture in the atmosphere (Illari 1989). Moreover, their useful coverage is restricted primarily to oceanic areas.

In summary, advantages of the satellite soundings available operationally today include good global coverage, high horizontal resolution, and, for the geostationary satellites, high temporal resolution (every hour, or even more frequently in special situations). Disadvantages include relatively low accuracies and low vertical resolution (compared to the radiosonde) and the interference of clouds and aerosols with the infrared radiances, which leads to contamination of the sounding or prevents the calculation of soundings below clouds altogether.

c. Commercial aircraft

Some commercial aircraft, through the Aeronautical Radio, Inc. Communication Addressing Reporting System (ACARS), provide thousands of accurate wind and temperature data daily to support operational weather prediction (Brewster et al. 1989). These data, however, are generally confined to cruising altitudes (9–12 km) and flight paths of commercial aircraft. Observations are also taken on ascent and descent near major airports.

d. Summary of upper-air temperature observation errors

Table 1 shows the estimates of temperature error standard deviations of various observational systems used in the spectral statistical interpolation for the global spectral model at the National Centers for Environmental Prediction [NCEP, formerly the National Meteorological Center (NMC)] as of June 1995 (J. Derber 1995, personal communication). They are derived from a combination of careful comparisons among observing systems, precision tests of instruments, and educated subjective estimates based on experience. These error estimates include both the random instrument error and sampling errors that arise from unrepresentativeness of a single measurement (due to small-scale atmospheric variability). For this reason, and because these error estimates are *tuned* to give the best results with this particular forecast model, they are generally higher than the absolute measurement errors associated with a particular instrument or system. Another contribution to the relatively high satellite temperature errors (compared to the error estimates of 1°–2°C quoted earlier) is that the satellite temperature errors are correlated in space rather than being random, independent observations. Thus, it is the relative (to each other) size of the errors shown in Table 1 that is important. We see in Table 1 that the greatest temperature errors are in the upper troposphere and lower stratosphere where GPS limb sounding temperatures are likely to be most accurate. This suggests that the use of GPS limb sounding temperature observations in this region have the potential to significantly improve the global analyses of temperature and the operational global forecasts.

4. Characteristics of GPS limb sounding

The potential strengths of GPS limb soundings include all-weather global coverage, high vertical reso-

TABLE 1. Observation temperature error standard deviations used in spectral statistical interpolation for the Global Spectral Model at NCEP, June 1995.

	Temperature errors (°C)					
Observational system	**1000 mb**	**700 mb**	**500 mb**	**300 mb**	**100 mb**	**50 mb**
Radiosonde	1.8	1.3	1.3	2.0	3.1	4.0
Aircraft reports	2.7	2.7	2.9	3.4	4.6	4.6
Dropsondes	1.8	1.3	1.3	2.0	3.1	4.0
ACARS	1.8	1.3	1.3	2.0	3.1	4.0
Satellite clear skies	4.7	3.9	4.0	4.5	4.0	4.0
Satellite cloudy skies	5.6	4.6	4.6	5.0	4.5	4.5

lution, high accuracy, high long-term stability, and cost effectiveness. A description of GPS and GPS limb sounding inversion methodology is included in the appendix.

A single GPS/MET satellite could provide roughly 500 refractivity soundings per day, through clouds and aerosols, with global coverage repeated every 12 h. From these refractivity soundings, valuable information on temperature or water vapor profiles can be derived. Hardy et al. (1992) estimate that soundings can be obtained beginning from about 60-km altitude and extending downward nearly to the surface over water and most land areas. Figure 2 shows the global distribution of soundings produced during one day by the *MicroLab 1* satellite in the GPS/MET experiment. The number of soundings shown is less than the maximum possible of roughly 500 per day because of 1) antenna-pointing and memory limitations for the *MicroLab 1* satellite, 2) the requirement for simultaneous tracking of the occulting GPS satellite by the LEO receiver and one of the five high-rate ground-based GPS tracking stations (described in the appendix), and 3) only setting (and not rising) occultations were observed.

The vertical resolution of several hundred meters to 1 km gives GPS limb sounding an advantage over most space-based atmospheric sensors. In particular, the radio occultation method provides vertical resolution comparable to the best limb sounders and significantly better than nadir-viewing satellite radiometers. On the other hand, GPS limb soundings represent an average measurement over a horizontal distance of several hundred kilometers, whereas the horizontal resolution of satellite radiometers is generally 20 km or less.

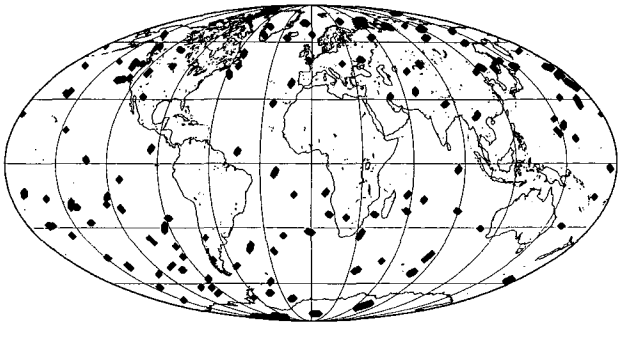

FIG. 2. Locations of GPS/MET soundings obtained during 7 h on 23 June 1995. Vertical soundings appear as single diamonds, and oblique soundings appear as a connected series of diamonds. Fewer than the maximum possible number of 500 daily soundings were observed because of satellite and tracking network limitations.

GPS/MET measurements enjoy inherently high precision because they are fundamentally carrier *phase* measurements made in a high signal to noise ratio (SNR) environment, except in the lower troposphere. This in turn results in a phase delay dynamic range of approximately 10^6. In contrast, all passive radiometers, limb and nadir pointing, rely on signal *amplitude* measurements made in a comparatively low SNR environment, resulting in lower dynamic range.

One of the most elegant and attractive features of the GPS/MET instrument is its inherent stability. There is literally *nothing* in the instrument itself requiring adjustment or calibration once the satellite is in orbit and in operation. GPS satellite and GPS/MET receiver positions with an accuracy of roughly 1 m are needed, but this has been easily attained using currently existing software and readily available global GPS tracking data (Zumberge et al. 1994). The GPS phase is referenced to a ground-based hydrogen maser with $\Delta f/f < 10^{-14}$ over 100 s. In contrast, space-based radiometers often require frequent in-orbit calibration, typically by measuring first the brightness temperature of deep space (2.7°C) and then a warm target on the spacecraft, monitored by platinum resistance thermometers. For example, the NOAA MSUs flown on the TIROS series required a separate calibration for every Earth scan.

Perhaps the single most intriguing characteristic of GPS limb sounding is its ability to leverage so effectively the multibillion dollar investment in GPS and commercial GPS receiver technology. No other space-based atmospheric sounding instrument even approaches the combination of small size, low mass and power, low cost of the GPS/MET payload, and all solid-state reliability. Future instruments, driven by the demand for high-performance commercial receivers, may be so small and affordable that their use will be limited only by the capacity of the ground segment to process and use the data. If the projected performance can be realized, these characteristics make constellations of GPS limb sounders economically feasible and capable of providing thousands of soundings daily.

Weaknesses of the GPS/MET measurement system include an ambiguity in the signal between temperature and water vapor, and errors introduced by multipath effects. The long horizontal averaging distances imposed by limb scanning (Fig. 1) can be either a strength or a weakness, depending on the application. Using geometric optics, each sample of occultation data can be associated with a point in space known to within a few meters, representing a mov-

ing average in the horizontal dimension of several hundred kilometers. The cross-beam resolution is approximately the same as the vertical resolution. Although long horizontal averaging distances may limit the application of GPS limb sounding for small-scale applications, horizontal averaging may increase the value of the method for large-scale weather and climate applications.

No existing single observational system can fully determine the global atmospheric temperature and water vapor structure. Every existing system has strengths and weaknesses regarding accuracy, spatial and temporal resolution, representativeness of volume sampled, and cost. However, many of the strengths and weaknesses of GPS limb sounding are complementary to those of other space- and ground-based sensors. Ongoing research should be focused on the question of how to best assimilate GPS limb sounding information so as to exploit its strengths and on the use of complementary systems in areas where it is weak. For example, a sounding with high horizontal and vertical resolution could be obtained by combining a GPS limb sounder and nadir radiometer.

5. Accuracy of temperature and water vapor profiles

When a GPS satellite, as viewed from the GPS/MET receiver, rises or sets, the GPS signal arrival time is delayed because of the refractive bending and slowing of the signal as it passes through Earth's atmosphere. As discussed by Melbourne et al. (1994a) and summarized in the appendix, the bending angle of the ray can be calculated from this delay. Further, the vertical profile of atmospheric refractivity can be calculated from the bending angles. Errors in refractivity arise from a number of sources, including 1) reference oscillator frequency drift in the LEO, GPS satellite, or ground-based GPS tracking receivers; 2) errors in receiver tracking; 3) precision orbit determination; 4) ionospheric effects that are not corrected by the dual-frequency phase measurements; 5) tracking errors due to multipath effects in the lower troposphere; and 6) departures from the atmospheric spherical symmetry assumed in the current inversion algorithms.

The relationship between refractivity, temperature, and water vapor is given by Eq. (A8) in the appendix. It follows that the temperature may be computed from known values of pressure P, refractivity N, and water vapor pressure e, as

$$T = \frac{77.6P + \left[6022.0P^2 + 14.92(10^5)eN\right]^{1/2}}{2N}, \quad (1)$$

where P and e are given in millibars and T is in Kelvins. Alternatively, if temperature is known, the water vapor pressure is given by

$$e = \frac{T^2N - 77.6PT}{3.73(10^5)}. \quad (2)$$

Several theoretical estimates of the temperature error resulting from reasonable estimates of the basic measurement errors listed above have been made assuming a dry atmosphere [$e = 0$ in Eq. (1)]. Neglecting ionospheric and humidity effects, Melbourne et al. (1994a) estimate that the temperature error increases exponentially with height from less than 0.1°C near the surface to 1°C at 50 km (because of the neglect of the ionosphere and water vapor, these are lower-bound estimates). More realistic simulations (Melbourne et al. 1988) indicate that the temperature errors between 5–7 and 40 km, where moisture effects are negligible, should be less than 1°C. Gorbunov and Sokolovskiy (1993) performed simulations with a global atmospheric circulation model and found temperature and geopotential height errors of 0.3°C and 3 m, respectively, at equivalent altitudes, with significantly larger errors near the surface. Simulations using the UCAR inversion code that produced the temperature profiles in this paper agree closely with these earlier estimates.

We may estimate the relationship between errors or uncertainties in temperature and water vapor pressure by differentiating Eq. (2) under the assumption of no errors in N or P:

$$\Delta e \approx \frac{(2TN - 77.6P)}{3.73(10^5)}\Delta T. \quad (3)$$

For typical values of $N = 300$, $P = 1000$ mb, and $T = 273$ K, we have

$$\Delta e \approx 0.23\Delta T, \text{ or } \Delta T \approx 4.35\Delta e. \quad (4)$$

From Eq. (1) we see that the neglect of moisture produces a cold bias in the derived temperature. We can use Eq. (4) to estimate the errors associated with

deriving water vapor profiles from known values of refractivity and independently estimated temperatures, or vice versa. Specifically, water vapor pressure can be estimated using in situ sensors to within 0.5 mb if temperature is known to within 2°C. This would be a useful estimate of water vapor over much of the lower atmosphere, where e typically varies between 5 and 20 mb and measurement or sampling errors of water vapor pressure are often greater than 1 mb. It may be more difficult to obtain useful temperature estimates given independent estimates of water vapor pressure, since e would have to be known to at least 0.23 mb (averaged over several hundred kilometers) to obtain temperature estimates accurate to within 1°C. Thus, the accuracy of moisture profiles will depend on the accuracy with which the temperature profile can be modeled or measured by independent means. Hajj et al. (1994) estimated that the error in relative humidity below 6 km will be less than 10%, providing that the temperature error is less than 2°C.

6. Spatial coverage and resolution

Spatial coverage is primarily a function of the GPS/MET spacecraft orbit. A simulator capable of predicting occultations as a function of the LEO orbit has been used to study a variety of orbits between 700 and 1000 km with inclinations from 45° to 99°. For the case of a single LEO receiver in a 900-km sun-synchronous polar orbit (and 24 GPS satellites), approximately 670 occultations per day will take place. Of these, approximately 500 would have geometry favorable for useful soundings with fore- and aft-viewing GPS antennas. By optimal selection of the orbit, it is possible to obtain a roughly uniform distribution over the entire surface of the earth. The GPS limb sounding technique will work equally well over water and land areas. In mountainous regions, profiles will not be available wherever the ray path is below the top of the terrain. Actual GPS/MET sounding locations for a 7-h period on 23 June 1995 are shown in Fig. 2.

Vertical and cross-beam resolutions are defined primarily by Fresnel diffraction and are expected to be several hundred meters near the ground increasing to 1 km near 60-km altitude (Melbourne et al. 1994a) with possible higher vertical resolution using Fresnel deconvolution. Along-path resolution will be 200–300 km (Kursinski et al. 1993). Recovered parameters represent weighted averages across the sampling volume. The vertical resolution is significantly better than that available from space-based *nadir*-viewing radiometer instruments. Moreover, the sampling volume center is known much more precisely, limited primarily by horizontal atmospheric inhomogeneities and differences in bending angles for the dual-frequency GPS signals. The vertical sampling interval is determined by the GPS/MET carrier phase sampling rate of 50 Hz. Since a typical occultation scans 60 km in altitude in approximately 60 s, the average vertical sampling interval is about 20 m. The high *vertical* resolution for GPS limb soundings and high *horizontal* resolution for nadir radiometric soundings could be combined. Bengtsson et al. (1995) simulated concurrent processing of data from both sounding methods and achieved a factor of 2 reduction in residual GPS limb sounding error.

7. Proof of concept experiment

The first GPS/MET observation was carried out on 16 April 1995, 13 days after the successful launch of *MicroLab 1*. The first inversion of this observation, which is located over Ecuador about 150 km from Guayaquil, is shown in Fig. 3. The data were inverted under a number of simplifying assumptions, including the neglect of water vapor, the use of 1-Hz averages of the 50-Hz GPS/MET receiver data, and a simple linear combination of the dual GPS frequencies for ionospheric correction. In spite of these simplifying assumptions, the sounding showed considerable realism compared to the standard U.S. tropical atmosphere model for April and agreed remarkably well with the closest radiosonde, which was located 500 km northeast of the GPS sounding. The neglect of water vapor causes the cold bias in the GPS/MET sounding below about 8 km in Fig. 3.

Figure 4 shows four representative GPS/MET temperature retrievals compared to nearby radiosonde data and to the temperatures provided by the NCEP global analysis, interpolated in time and space to the location and time of the GPS/MET sounding. In these comparisons, the GPS/MET temperature retrievals are calculated assuming a dry atmosphere, as discussed earlier; this assumption causes a cold bias in the lower troposphere where water vapor becomes an important effect.

The soundings in Fig. 4a correspond to a location near Port Harrison, Canada (which is in the extreme northwestern portion of the province of Quebec). The GPS/MET temperatures, the temperature from the

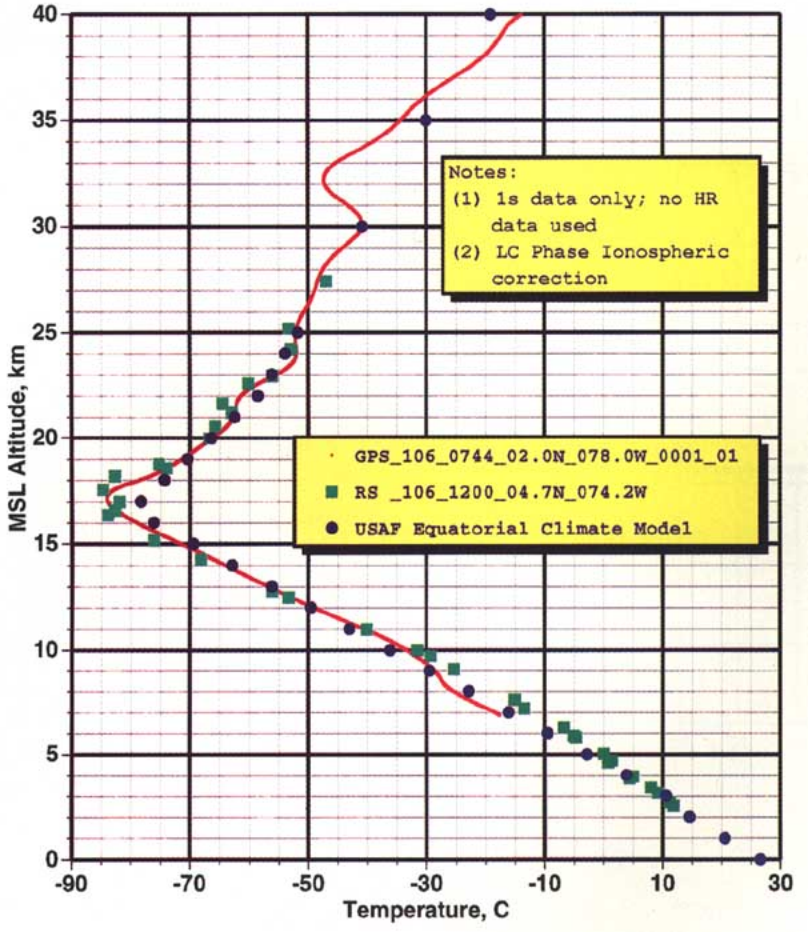

FIG. 3. The first inversion of a GPS/MET sounding, completed 26 April 1995. The observation occurred 16 April 1995 over Ecuador. The U.S. Air Force (USAF) tropical atmosphere model and nearby radiosonde (RS) profiles are also shown.

nearby radiosonde (approximately 100 km away in space and 3 h in time), and the temperatures from the NCEP analysis agree to within about 3°C from about 31 (the highest altitude reached by the radiosonde) to 5 km (the lowest altitude reached by the GPS/MET sounding). The GPS/MET sounding shows high vertical resolution and provides an excellent estimate of the location and temperature minimum of the tropopause. The complex structure of the temperature profile at and near the tropopause, in which the profile shows a *kink* feature consisting of a weak local maximum of temperature above the tropopause followed by a further decrease of temperature with height is seen in many of the GPS/MET soundings and, to the extent that this structure is revealed by the lower-resolution radiosondes and the NCEP analysis, appears to be real.

The sounding in Fig. 4b, located near Freiburg, Germany, shows that the GPS/MET temperature sounding matches six nearby radiosondes quite well from 31 to about 7 km and again resolves the tropopause very well. From 6 to 3.5 km, neglect of the effect of water vapor causes a cold bias of approximately 8°C in the GPS/MET sounding.

The sounding shown in Fig. 4c, which is over the Aleutian Islands southwest of Anchorage, Alaska, agrees well with the nearby radiosonde and with the NCEP analysis from 26 down to 3 km. Below 3 km, the retrieved temperatures indicate the receiver probably encountered strong defocusing and/or multipath. In general, these early GPS/MET retrievals have difficulty getting below 5 km, probably due to a number of difficulties associated with the evolving inversion algorithms, defocusing of the GPS signal by atmospheric lens effects, multipath, receiver cycle slips and loss of lock, and possible terrain effects.

Figure 4d shows a sounding in the Southern Hemisphere, near Adelaide, Australia. Again, the GPS/MET retrieval matches the two nearby radiosonde soundings and the NCEP analysis well and also captures the complex temperature structure at and above the tropopause.

Figure 5, a sounding that reaches downward to about 1 km above the surface over the Kamchatka Peninsula, shows the pronounced effect of water vapor in the lower troposphere. A rough calculation using Eq. (3b) shows that the cold bias of approximately 17°C at 1 km corresponds to a water vapor pressure of 4 mb. This estimate agrees fairly well with the observed value of approximately 5.0 mb as estimated from the two nearby radiosondes. The kink feature in the tropopause is well depicted by the GPS/MET sounding in Fig. 5.

Figure 6 shows a GPS/MET retrieval over Charleston, West Virginia, compared to three nearby radiosondes, the NCEP analysis, and two high-resolution research radiosondes. As in the previous examples, the GPS/MET retrieval agrees well with the other soundings in the upper troposphere and stratosphere where water vapor effects are negligible. Of note in Fig. 6 is the presence of vertical oscillations in the tempera-

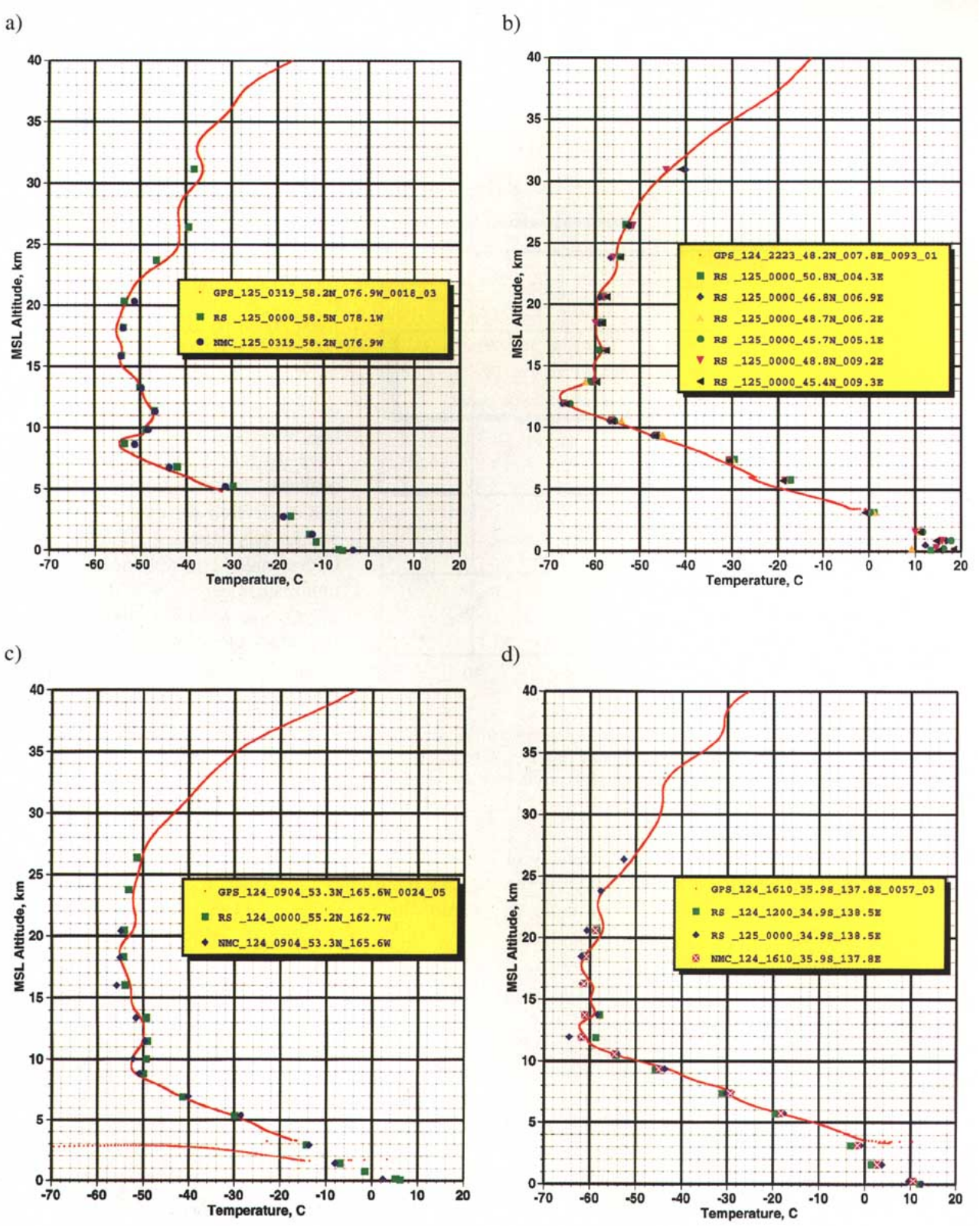

FIG. 4. GPS/MET soundings observed (a) 5 May 1995 over northwest Quebec, east of Hudson Bay and on 4 May 1995 (b) near Freiburg, Germany; (c) over the Aleutian Islands southwest of Anchorage, Alaska; and (d) near Adelaide, Australia. GPS antispoofing (A/S) was off, and a dry atmosphere was assumed. Also shown are nearby radiosonde (RS) and interpolated profiles from the NCEP analysis. The discontinuous dotted curve below 3 km in (c) is probably caused by loss of lock and/or multipath in the GPS/MET data.

ture profile on the scale of 2 km between 10 and 20 km in the high-resolution soundings, confirming the same scale of oscillations in the GPS/MET retrieval. The high-resolution soundings also show vertical oscillations on a scale of a few hundred meters, which do not appear in this analysis of the GPS/MET sounding.

Figure 7 shows another comparison (over South Dakota) with high-resolution balloon data. This GPS/MET retrieval captures the vertical temperature structure well but shows a cool bias throughout most of the sounding compared to three high-resolution soundings and one radiosonde, all launched 5 h before the GPS/MET sounding. The agreement is close to the other radiosonde, launched 7 h after the GPS/MET sounding, and to the NCEP analysis, which is interpolated to the location and time of the GPS/MET sounding. The cool bias may be attributed to the 5 h of cold advection that occurred following the earlier soundings. The GPS/MET sounding in Fig. 7 again indicates the difficulty in the retrieval process below about 7 km.

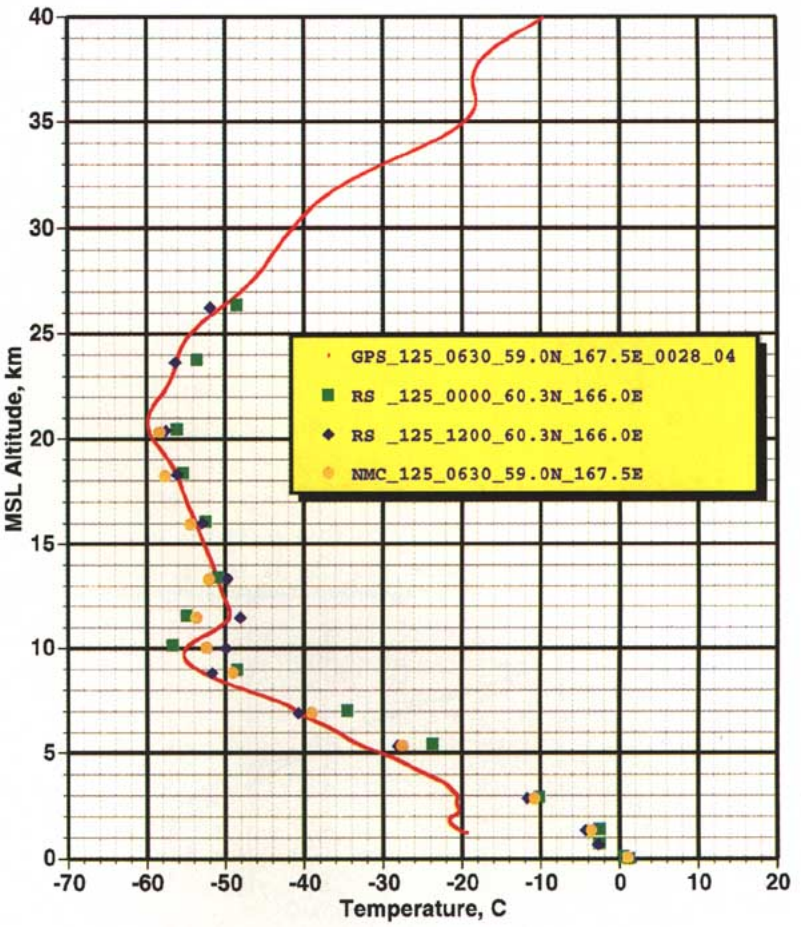

FIG. 5. GPS/MET sounding observed 5 May 1995 over the Kamchatka Peninsula, Russia. The cool GPS/MET temperature bias in the lower troposphere is due to atmospheric moisture. Also shown are nearby radiosonde (RS) and interpolated profiles from NCEP analysis.

Figure 8 shows a comparison of a GPS/MET sounding over western Lake Superior with two high-resolution balloon, two radiosonde soundings, and the NCEP analysis. As in previous soundings, the GPS/MET sounding shows excellent agreement with the other data.

Figure 9 shows a GPS/MET sounding over northwestern China (northwest of Beijing) compared to 10 radiosondes and the NCEP analysis. This figure gives a good idea of the range of variability of radiosonde temperature profiles due to the combined effect of different radiosonde errors and variations due to differences in location and time; the typical range of temperatures among the 10 radiosondes is 5°C with some differences exceeding 10°C. The GPS/MET sounding tends to run through the middle of the 10 radiosondes, except in the lower troposphere where moisture effects are important.

Figure 10a depicts a sounding, located over Parkersburg, West Virginia, with a pronounced kink in the temperature profile above the tropopause. That this kink in the GPS/MET retrieval is real is demonstrated by two high-resolution soundings taken 4 h earlier. The vertical structure in the region of the tropopause is highlighted in Fig. 10b, which enlarges the soundings in Fig. 10a between 9 and 19 km. The agreement between the GPS/MET sounding and the closest high-resolution sounding is remarkable.

Figure 11 compares preliminary temperature retrievals in the upper part of the stratosphere from GPS/MET and the Halogen Occultation Experiment (HALOE). Here, there are no radiosonde or NCEP data. We found one occultation that was reasonably close in space and time to a temperature retrieval from the HALOE instrument, carried on the *Upper Atmosphere Research Satellite*. HALOE measures the attenuation of solar radiation as the sun rises or sets relative to the satellite. The HALOE sounding shows a smooth and realistic variation of temperature with

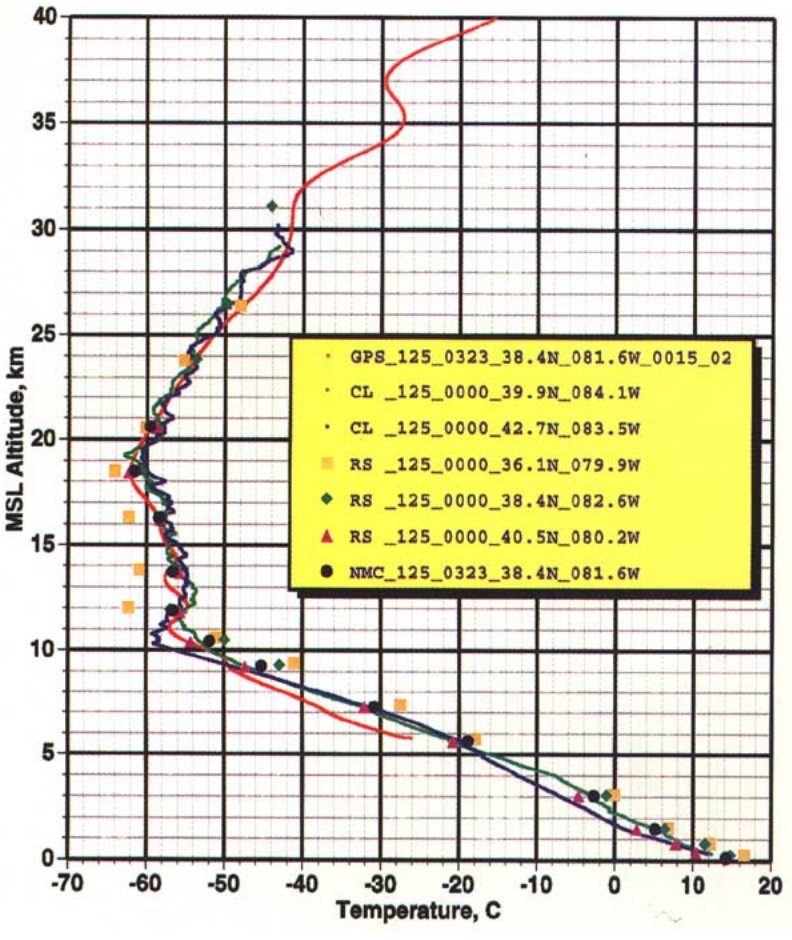

FIG. 6. GPS/MET sounding observed 5 May 1995 near Charleston, West Virginia. Also shown are high-resolution radiosonde temperature profiles (CL), radiosonde (RS), and interpolated profiles from NCEP.

height, with a maximum around 45 km. In contrast, two GPS soundings, which differ in the use of ground-based GPS tracking stations (see appendix), show unrealistic, large oscillations above 40 km with respect to the HALOE data. These oscillations, and the differences between the two soundings, appear to be related to boundary conditions at the initialization point for the retrieval inversion algorithm in the upper atmosphere. Future refinements in boundary condition modeling may reduce the oscillations. In any case, the two solutions damp exponentially with decreasing elevation and converge below about 40 km.

8. Scientific uses of GPS limb sounding data

GPS limb sounding data have the potential to be applied in the high-priority areas of weather forecasting and climate research. The potential contribution of GPS limb sounding data to these scientific areas is discussed below, followed by a brief description of some of the other areas of science that may ultimately benefit from the availability of GPS occultation data.

a. Weather analysis

GPS limb sounding could lead to significant improvements in operational weather forecasting by providing high-resolution temperature and moisture data on a global basis, complementing existing in situ and remote sensing observations. Section 3 described the strengths and weaknesses of the radiosonde, satellite, and commercial aircraft observations. GPS limb sounding has the potential to build upon the strengths of these systems and contribute to better observational coverage in both time and space with good vertical resolution of temperature and moisture over both oceans and continents, thereby improving the accuracy of numerical four-dimensional data assimilation analyses.

Although GPS limb soundings have the potential to enhance the analysis and prediction of weather and climate, significant research is required to assess this potential in detail and develop capabilities to derive maximum benefit from this new source of atmospheric data. Fundamental studies are needed to 1) quantify the accuracy of retrieved temperature and moisture profiles for the spectrum of real atmospheric conditions that will be encountered, 2) determine how these data can be most effectively used by weather forecast models, and 3) enhance the accuracy and resolution of the data by combining these models and other data sources with the retrieval process. In addition, data acquisition in the lower troposphere is currently degraded by defocusing and multipath, and improved tracking strategies and algorithms are needed.

Preliminary simulations indicate that the optimum way of using GPS limb sounding data in numerical weather prediction models may be to assimilate more fundamental observables, such as refractivity profiles or even bending angles (Eyre 1994), directly into the model rather than assimilating temperature and water

vapor profiles derived from the refractivity profiles (Zou et al. 1995). Zou's approach minimizes the difference between a model prediction and the observed profile of refractivity in a certain time window.

b. Global change research

Although there is consensus in the scientific community that climate change is likely as a result of the observed increases in greenhouse gases in the atmosphere (Houghton et al. 1990, 1992), there is much uncertainty about the magnitude and details of the change. Thus, there is a great need for better observational data to document the climate and how it is changing with time. The need is for both regional and global monitoring of many climatological variables.

A long record of GPS limb sounding observations could have a significant impact on climate and global change issues. One of the signals expected from the increases in greenhouse gases from anthropogenic sources is in global mean temperature. However, detection of the expected lower-tropospheric global warming is confounded by flawed and patchy observations, by natural variability that adds climatic noise to the system, and because observed climate change is not geographically uniform. Therefore, although there are clearly established upward trends in several greenhouse gases, it has not yet been possible to establish unequivocally that the approximately 0.5°C increase in global surface temperatures observed over the last century is caused by increases in greenhouse gases.

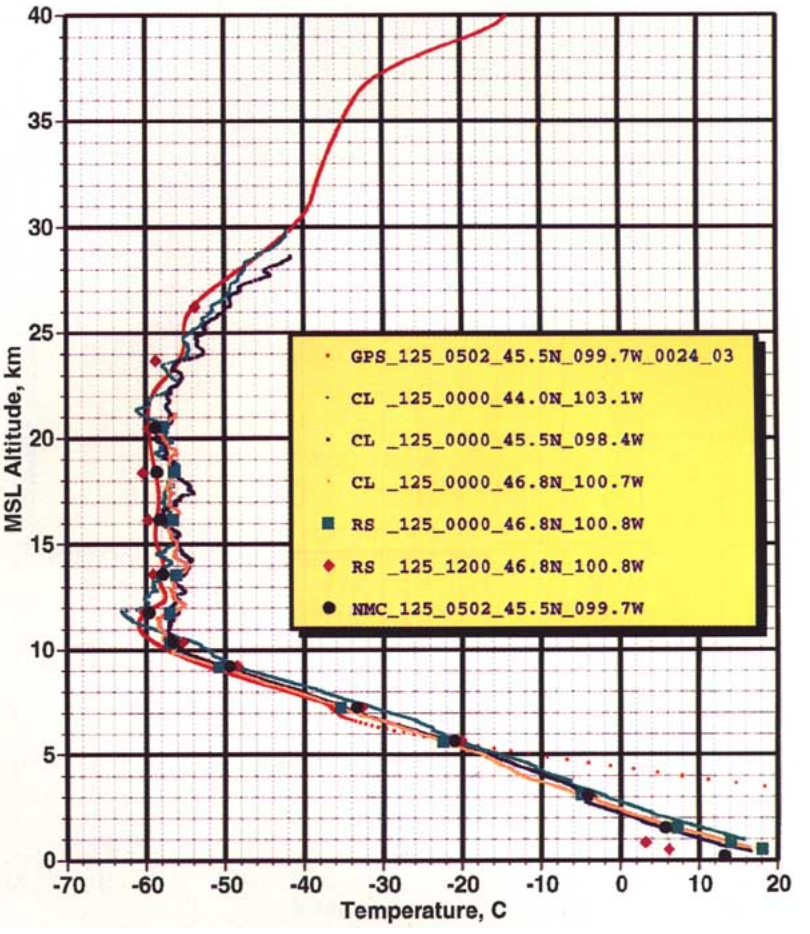

FIG. 7. GPS/MET sounding observed 5 May 1995 over South Dakota. The erratic behavior of the GPS/MET profile below about 7 km may be a result of defocusing of GPS signals by atmospheric gradients. Also shown are nearby high-resolution balloon (CL), radiosonde (RS), and interpolated profiles from the NCEP analysis.

An important indicator of climate change associated with temperature change is an expected increase in water vapor (Rind et al. 1991; Gaffen et al. 1992). Water vapor itself is also a strong greenhouse gas, providing feedback effects that can substantially enhance temperature changes. Increases in greenhouse gases are expected to warm the lower troposphere and cool the stratosphere, with the amount of cooling increasing with height to at least 30 km (10 mb).

The detection of any greenhouse gas–induced temperature trends in the stratosphere is compounded by the very large natural variability there. This variability is associated with the stratospheric quasibiennial oscillation, decadal timescale changes associated with solar activity (Van Loon and Labitzke 1990), sudden stratospheric warmings, and the effects of changes in ozone concentrations. In addition, the observational record is limited at most to four decades. Therefore, it has not been possible to detect a greenhouse gas signal in stratospheric temperatures. Nevertheless, global long-term GPS limb sounding measurements of stratospheric temperature may be useful for global climate research.

A related global change issue is the loss of ozone in the stratosphere arising from the increases in human-made chlorofluorocarbons (CFCs). CFCs are essentially inert in the troposphere but break down in the stratosphere and lead to depletion of ozone through complex heterogeneous chemistry. The most pro-

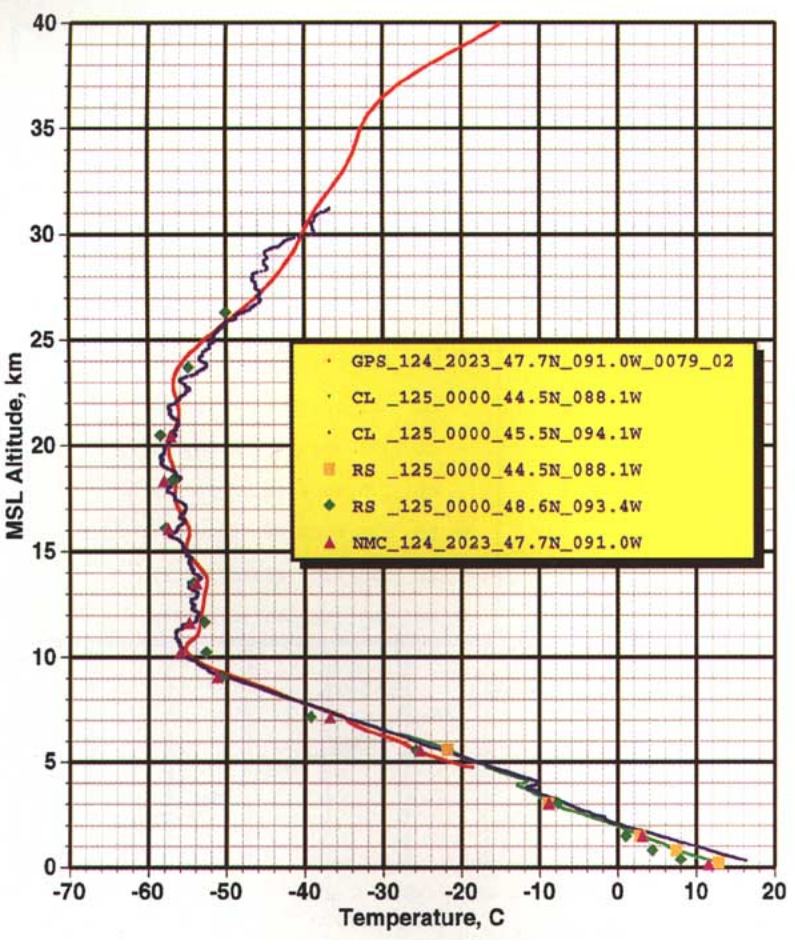

FIG. 8. GPS/MET sounding observed 4 May 1995 over western Lake Superior. Also shown are nearby high-resolution balloon (CL), radiosonde (RS), and interpolated profiles from the NCEP analysis.

nounced example of this is the emergence of the ozone hole at high latitudes during the spring in the Southern Hemisphere. Stratospheric temperatures are very critical to this process, as the polar stratospheric ice cloud particles, which play a key role in facilitating the chemical reactions leading to ozone depletion, form mainly at very low temperatures. Stratospheric cooling from increases in greenhouse gases may exacerbate ozone losses. Improved understanding of temperature changes in the stratosphere, important for global change research, could be accomplished using GPS limb sounding data.

As discussed in section 5c and the appendix, ancillary data from other sources usually will be required to derive either temperature or moisture profiles from GPS occultation data. However, profiles of atmospheric refractivity are retrieved directly from GPS occultation data. Since refractivity is a function of atmospheric temperature and moisture and these variables have been identified as key indicators of global change, it may be possible to interpret refractivity profiles as a "holistic global change indicator."

Model results support the conclusion that refractivity profiles could provide a useful parameter to measure long-term changes and trends in the global atmosphere. Using the National Center for Atmospheric Research Community Climate Model and ray tracing tools, Yuan et al. (1993) demonstrated that the change in refractivity resulting from a doubling of atmospheric CO_2 would be significant. This finding is important since refractivity profiles derived from GPS limb soundings will generally be more accurate than the derived temperature or moisture profiles.

Moreover, as illustrated in Fig. 12, Yuan et al. (1993) found that the total raw GPS limb sounding propagation delay measured as a function of height may provide an even more fundamental integrated signal of global change. If temperature and moisture increase with global warming, the total propagation delay will also increase, providing another measure of global change.

Climate change has also been linked to volcanic activity. An injection of material from a large volcanic eruption can result in massive amounts of aerosol in the lower stratosphere, which significantly limit satellite infrared observations of this and lower regions. However, because these aerosols change the radiative forcing of the atmosphere, this is precisely the time and place where accurate observations are needed to determine how the atmospheric thermal structure is changing to achieve overall radiative energy balance. Unlike passive infrared radiometers, the accuracy of GPS limb sounding observations will be relatively unaffected by these aerosols.

c. Other research opportunities

GPS limb sounding technology also will provide an opportunity for global mapping of the ionosphere with sufficient temporal and spatial resolution to investigate many important dynamical processes in the ionosphere/thermosphere system and their relation to

processes in the atmosphere and solid Earth. For example, data from GPS limb sounding could be useful in the study of gravity waves, which transport energy and momentum through the neutral atmosphere and ionosphere. Tracing this phenomenon may be possible by mapping the total electron content (TEC) along the ray path between the LEO and GPS satellites. It has been estimated that the accuracy and precision of TEC derived in this way will approach 10^{15} and 10^{14} e m^{-2}, respectively (Melbourne et al. 1988). This accuracy corresponds to 0.1% of the daytime zenith peak in TEC. Information on global energy transport through the observation of gravity waves in the stratosphere could add further to the science objectives of global change research and weather forecasting.

As an example of another opportunity, adding a LEO GPS receiver to the growing *fiducial* network used for GPS precision geodetic surveys will improve the accuracy of all positions taken in ways not possible with an exclusively Earthbound fiducial network. This will occur primarily due to the improved GPS orbits obtained when the geometry of a fiducial network includes an orbiting receiver, as demonstrated for the TOPEX/POSEIDON satellite by Melbourne et al. (1994b). Improved GPS orbits will improve the accuracy of a variety of scientific applications of GPS (e.g., Ware and Businger 1995). For example, as shown by Malla et al. (1992), a detailed covariance analysis indicates that GPS will be more effective in the study of crustal deformation ". . . when data collected from low Earth-orbiting satellites as well as from ground sites are combined, enhancing the accuracy and resolution for measuring high frequency geophysical signals over timescales of less than one day."

Another opportunity follows from the fact that anisotropic turbulence in the horizontal atmospheric structure may cause considerable amplitude variations in the occultation signal (Dalaudier et al. 1994). Measurement of these fluctuations will allow determination of turbulence parameters responsible for vertical atmospheric diffusion.

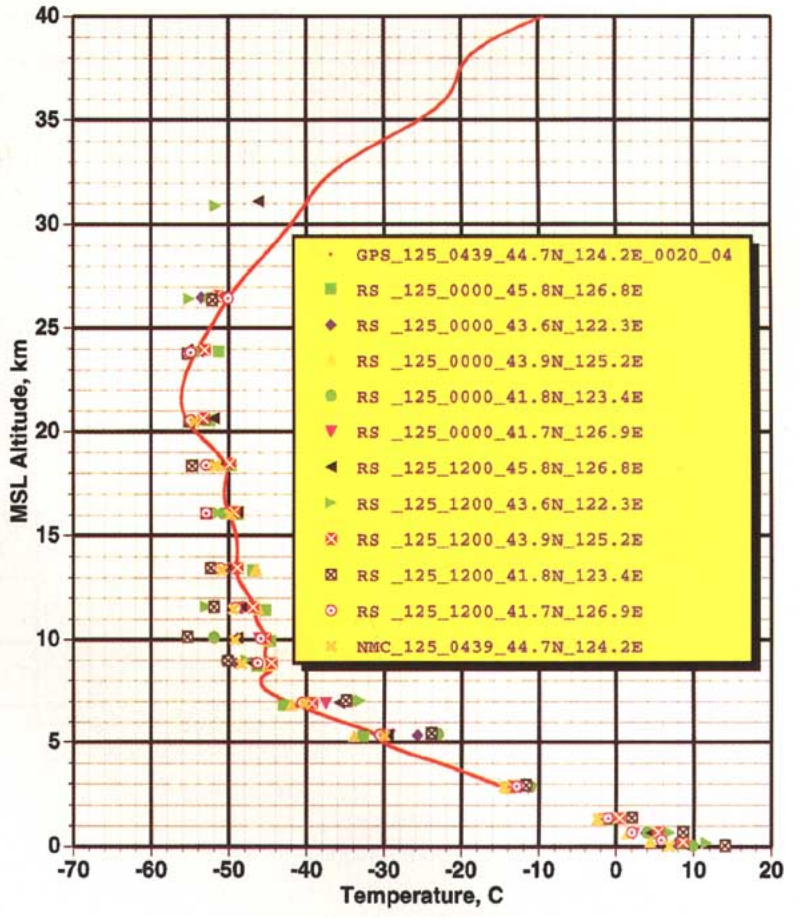

FIG. 9. GPS/MET sounding observed 5 May 1995 northwest of Beijing, China. Also shown are nearby radiosonde (RS) and interpolated profiles from the NCEP analysis.

In addition, accurate temperature profiles are needed as initial conditions for many existing and planned passive satellite remote sensing systems (e.g., humidity, ozone, other trace gases). GPS limb sounding could help provide these profiles.

Finally, the combination of GPS-sensed refractivity profiles (from space) and GPS-sensed precipitable water vapor data (from the ground) could be assimilated into four-dimensional models to improve the definition of temperature and moisture over continents.

9. Summary

Preliminary results show that accurate vertical temperature profiles from an altitude of approximately 40 to about 5 km can be obtained using the GPS limb sounding technique. GPS/MET-derived temperatures in this region usually agree within 2°C with tempera-

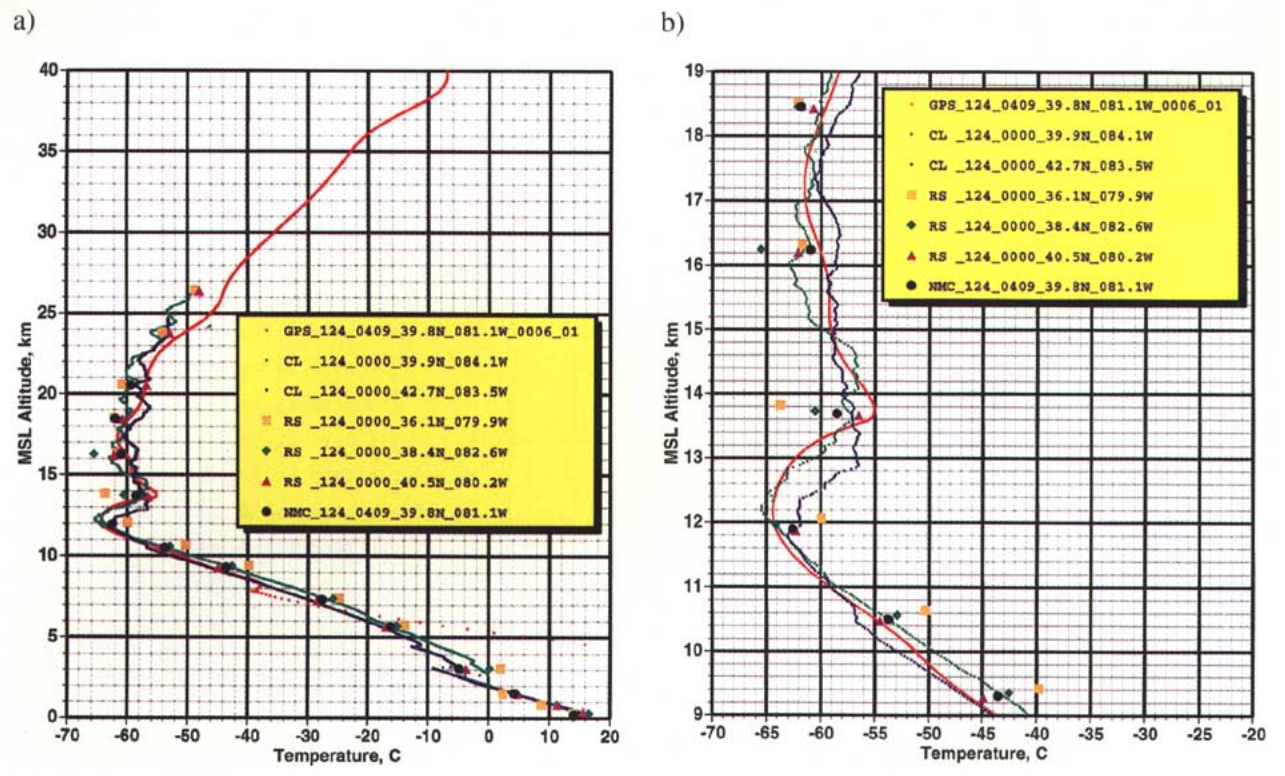

FIG. 10. GPS/MET sounding observed 4 May 1995 near Parkersburg, West Virginia: (a) regular and (b) expanded view from 9- to 19-km altitude. Erratic behavior of the GPS/MET profile below about 8 km may be a result of defocusing of GPS signals by atmospheric gradients. Also shown are nearby high-resolution balloon (CL), radiosonde (RS), and interpolated profiles from the NCEP analysis.

tures measured by nearby balloon soundings and with temperatures interpolated in time and space from the NCEP analysis. GPS/MET profiles have a vertical resolution of about 1 km and routinely resolve the location and the temperature of the tropopause.

Data above 40 km and below 5 km from these preliminary GPS/MET analyses require improved interpretation. In the upper atmosphere, the major difficulties are associated with the upper-atmosphere boundary conditions and possibly with the ionosphere. In the lower troposphere, the problems are probably linked to multipath effects caused by pressure, temperature, and water vapor gradients. These difficulties are being investigated.

Appendix: Background and theoretical aspects of GPS limb sounding observations

a. GPS characteristics

GPS includes 24 operational satellites, four in each of six 12-h 20 000-km circular prograde orbits, all inclined 55° to produce global coverage. The GPS satellites transmit two L-band carrier frequencies: 1575.42 (L1) and 1227.6 MHz (L2). Each carrier is phase modulated by a precise ranging code (P-code) consisting of pseudorandom bit sequences at 10.23 Mb s^{-1}. In addition, the L1 carrier is modulated with a 1.023-Mb s^{-1} pseudorandom bit sequence used for the coarse (or clear) acquisition code (C/A-code). The transmit time, as kept by the clock onboard each GPS satellite, is precisely known for each bit in the sequence. A GPS receiver identifies the incoming code bits and measures their arrival time, as kept by the receiver clock, with a precision of better than 1% of a bit length (about 1 ns or 30 cm for the P-code). A priori GPS orbital positions and clock offsets between GPS satellites are broadcast to the user along with other information on a 50-bps data message superimposed on the L1 and L2 carriers. The difference between the known transmit time and observed arrival time is a measure of the distance between the satellite and receiver plus the clock offset between transmitter and receiver clocks, a quantity referred to as *pseudorange*. A receiver simultaneously measuring pseudoranges to four satellites can instantaneously de-

termine its three components of position and its time offset from GPS time, typically with an accuracy of 10–15 m and better than 1 μs, respectively. Modern receivers can also measure and keep continuous count of carrier phase with a precision of better than 0.5% of a wavelength (approximately 1 mm). Continuous phase can then be used to construct a record of *position change* with millimeter precision.

For reasons of national security, current U.S. government policy calls for limiting access to the Precision Positioning Service (PPS) and the accuracy of the Standard Positioning Service. Two techniques are used to limit the access and the accuracy of GPS: selective availability (S/A) and/or antispoofing (A/S). The A/S technique is a process used to deny users access to the full capabilities of the system by encryption of the high-rate P-code normally required for high-precision measurements. When so encrypted, the high-rate code is referred to as the Y code. Unless the user has the required encryption key to track the Y code, the user will not have access to the PPS. The S/A technique is believed to involve the deliberate introduction of small, random errors in the broadcast satellite ephemeris data and in the transmitted carrier and/or clock frequency. Uncorrected, S/A can result in position errors on the order of 100 m.

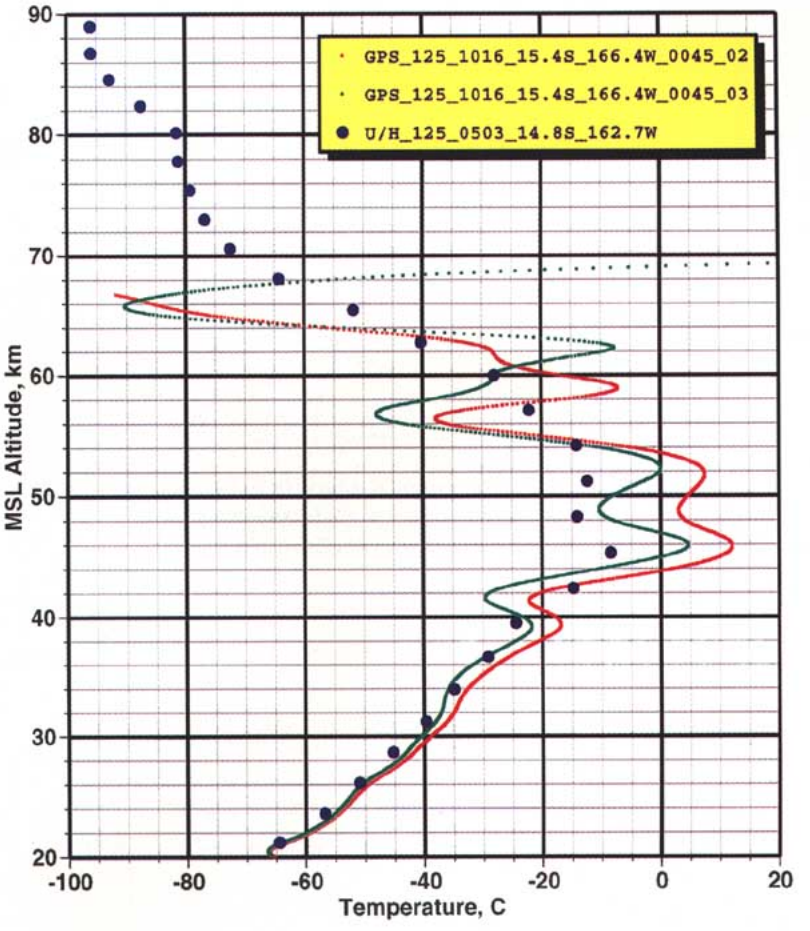

FIG. 11. Two retrievals are shown for a single GPS/MET measurement on 5 May 1995 near Western Samoa in the South Pacific. Each used a different GPS fiducial tracking site. A temperature sounding from the Halogen Occultation Experiment is shown for comparison. We attribute the large oscillations in the GPS/MET retrievals and differences between them to differences in the assumed initial altitude and pressure conditions near 70 km.

The TurboRogue GPS/MET receiver uses a codeless option when A/S is on, and L2 carrier phase tracking is performed without explicit knowledge of the Y code. Most codeless techniques use the Y code residing on both the L1 and L2 carriers with cross or autocorrelation to recover full wavelength L2 phase. The penalty of using a codeless technique is minor when good SNR conditions prevail or when the phase dynamics of the tracked signal are sufficiently predictable so that signal averaging can be performed. Therefore, use of codeless techniques for recovery of full wavelength L2 phase (for altitudes of about 6–40 km) results in SNR-induced errors that are small compared to other error sources. However, for the lower troposphere where adverse SNR and signal dynamics prevail and in the upper stratosphere where SNR and ionospheric correction errors prevail, the use of high-gain antennas and Y-code receivers (when A/S is on) may be required to fully exploit the potential of GPS limb sounding.

A technique known as double differencing is employed in high-accuracy GPS geodesy to cancel most transmitter and receiver clock errors. By differencing observations of a given GPS satellite at two receivers, clock errors and S/A dithering for that satellite are canceled. This is referred to as a single difference (SD). If SDs are formed for a second GPS satellite and differenced with the first SD, a double difference is formed canceling errors common to the receiver clocks. If double differencing is used in conjunction with receiver clocks synchronized to better than 1 ms,

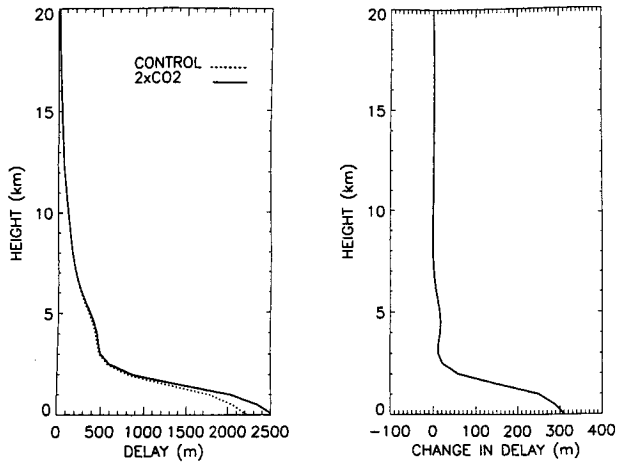

FIG. 12. Change in delay for tropical zone 10°S–10°N, averaged over the month of July, for climate model simulations of present-day and doubled carbon dioxide levels (Yuan et al. 1993).

S/A is effectively canceled, just as normal clock errors are canceled (Rocken and Meertens 1991). Therefore, A/S and S/A do not preclude the use of the GPS for occultation measurements.

For GPS/MET, ground-based data collected from precisely known 1-Hz GPS fiducial tracking sites are double differenced with the data collected from the GPS/MET LEO receiver. The tracking sites used for GPS/MET, located in Australia (Tidbinbilla), Alaska (Fairbanks), California (Pasadena), Germany (Potsdam), and Hawaii (Kokee Park), are part of the worldwide International GPS Service network.

b. Retrieval methodology

The process described below might be considered the *classic retrieval method.* The fundamental principles have evolved over time from the original planetary occultation work conducted at JPL and Stanford (described in section 2) and are similar to methods used in seismology (Phinney and Anderson 1968). A detailed description of the retrieval methodology offered below is provided by Melbourne et al. (1994a).

1) COMPENSATING FOR THE IONOSPHERE

To extract information on the neutral atmosphere, propagation delays caused by the ionosphere must be isolated and removed from the signal. Electrons in the ionosphere cause a *frequency-dependent* delay in the phase of received GPS signals. Anticipating the need for ionospheric corrections, GPS planners designed into the system the use of two carrier frequencies, L1 and L2, as previously described. By using *dual-frequency* phase measurements and knowledge of the inverse square relationship between the ionospheric group delay and the frequency of each carrier, a simple linear correction can be derived. According to a study conducted by Hajj and Kursinski (1991), a simple linear combination correction is accurate to 1 mm for nighttime occultations below 80 km. The error increases above 80 km. Because of high electron density variability in the daytime ionosphere, the simple linear combination correction is good only to 1–5 cm below 80 km, primarily due to splitting of the L1 and L2 rays. The required correction can be expressed as follows:

$$\Delta T_{L1} = 1.5336 \Delta T_{L1-L2}, \qquad \text{(A1)}$$

where ΔT_{L1} is the ionospheric time delay for L1 and ΔT_{L1-L2} is the measurable difference in delay between L1 and L2. The Doppler frequency offset, also affected by the ionosphere, can be modeled with a similar linear correction:

$$\Delta f_{L1} = 3.529\left(\Delta f_{L2} - \Delta f_{L1}\right), \qquad \text{(A2)}$$

where $(\Delta f_{L2} - \Delta f_{L1})$ is the measurable Doppler difference (Spilker 1978).

The dominant residual error of traditional ionospheric correction results from the different bending of L1 and L2 carriers (Hardy et al. 1993). To reduce this effect, Vorob'ev and Krasilnikova (1994) suggested a modified method of ionospheric correction based on a linear combination of separate refraction angles for the two carriers. This method, used in analysis of the results presented here, assumes the same impact parameter instead of the same time (the impact parameter is defined in the following section). Correcting for ionospheric effects completes the first step in the recovery of meteorological data from the GPS/MET observables.

2) RECOVERING ATMOSPHERIC INDEX OF REFRACTION

The fundamental measurement in the GPS limb sounding technique is phase delay resulting from transmission of the GPS signal through the atmosphere. Total atmospheric delay is a function of two factors: *ray bending* due to refraction and *reduced propagation velocity* in the atmosphere. The radio signal propagating from the GPS transmitter to the LEO receiver follows a path through the atmosphere that curves distinctively in response to atmospheric gradients in refractive index. The cumulative effect of the

atmosphere on the ray path can be expressed in terms of the total *refractive* bending angle α, which has a known relationship to the atmospheric Doppler shift. For Earth's atmosphere, the maximum bending angle is on the order of 0.03 rad (1.5°). The atmospheric Doppler shift is in turn determined by taking the time derivative of the observed phase. The variation of α with experiment geometry can be characterized through use of an *impact parameter a,* defined as the perpendicular distance between the center of the planet and the straight line followed by the ray approaching the atmosphere. When combined with a precise knowledge of the geometry (obtained concurrently from other GPS satellites), each sample of phase data (corrected for ionospheric effects) can be converted to the corresponding values for α and a. This step is straightforward and involves simple geometrical considerations, basic laws of geometrical optics, and relativistic formulas for Doppler shift.

For an atmosphere with local spherical symmetry (i.e., no significant asymmetric *horizontal* variations in temperature or moisture), and having determined the bending angle $\alpha(a)$ as described above, there is a unique relationship between $\alpha(a)$ and $\mu(r)$, the atmospheric refractive index as a function of radius r. The refractive index profile $\mu(r)$ is then derived through an Abel transform of the measurements of $\alpha(a)$ obtained over the complete occultation:

$$\ln \mu(r_o) = \frac{1}{\pi} \int_{a_o}^{\infty} \frac{\alpha(a)}{\left(a_o^2 - a^2\right)^{1/2}} da, \qquad \text{(A3)}$$

where a_o is the value of a for the ray whose radius of closest approach is r_o. Application of Eq. (A3) will provide the index of refraction profile through the atmosphere. This transformation assumes 1) the atmospheric shells are spherical and 2) each shell has a uniform index of refraction, that is, no horizontal variations.

The assumption of spherical symmetry is a limitation that must be overcome to achieve the generality desired for an operational system. Some state-of-the-art ray-tracing algorithms developed for seismology do not depend on this assumption.

c. Relationship of refractivity to meteorological parameters

Atmospheric parameters of interest can be derived from the refractive index profile through the following sequence of steps. To simplify the explanation, the process will first be described for the case of dry air. Then the effect of moisture will be considered.

1) Dry air case

First, as the index of refraction μ is close to unity in the terrestrial atmosphere, it is convenient to define the refractivity:

$$N = (\mu - 1)10^6. \qquad \text{(A4)}$$

For dry air, N can be expressed as

$$N = 77.6\frac{P}{T}, \qquad \text{(A5)}$$

where P is the pressure in millibars and T is the temperature in kelvins. Furthermore, by virtue of the equation of state, Eq. (A5) may be written as

$$N = 77.6\rho R, \qquad \text{(A6)}$$

where ρ is the air density in kg m^{-3} and R is the gas constant for dry air. Equation (A6) shows that ρ is directly proportional to N for dry air, so that $\rho(r)$ can be obtained easily from $\mu(r)$. Next, $P(r)$ can be obtained from $\rho(r)$ by integrating the equation of hydrostatic equilibrium:

$$\partial P/\partial z = -g\rho, \qquad \text{(A7)}$$

where z is the altitude and g is the acceleration of gravity. Finally, T can be obtained from P and ρ using the equation of state. In summary, for dry air, vertical profiles of ρ, P, and T can be obtained from $\mu(r)$ in a direct and simple manner.

2) General case

The procedure described above must be modified to account for the presence of water vapor. When the effect of water vapor is included, the expression for the refractivity is

$$N = 77.6\frac{P}{T} + 3.73\left(10^5\right)e/T^2, \qquad \text{(A8)}$$

where e is the vapor pressure of water in millibars. The first or dry term has been supplemented by a contribution from the second or wet term due to water vapor, which can be substantial in the lower troposphere. The wet term also exhibits considerable variation with location and time. The separate contributions

to N by the dry and wet terms cannot be distinguished uniquely through occultation measurements. This introduces an ambiguity into the profiles of ρ, P, and T; the effects of water vapor at variable and uncertain concentrations are indistinguishable from the effects of variations in temperature and pressure.

At altitudes above the tropopause, this ambiguity is not a significant problem as the contribution to the refractive index by water vapor is nearly always much less than 2%. Similarly, the contribution of moisture to refractive index is negligible throughout the polar atmosphere during winter. In the lower troposphere, ambiguity can be overcome. For example, if the temperature profile in the troposphere were known from model calculations, then moisture profiles could be retrieved from the measurements. This approach will work best in tropical regions where the temperature profiles exhibit relatively small changes, but moisture fields change significantly in space and time. It should be emphasized that μ and N can still be determined uniquely regardless of the abundance of water vapor.

Acknowledgments. Funding for the GPS/MET program was provided by the NSF, NOAA, the FAA, and NASA. Fundamental radio occultation methods used in the program were developed by the JPL and Stanford University scientists over the past three decades as a part of the NASA planetary exploration program. The JPL developed the TurboRogue receiver and the firmware used for GPS/MET. NASA supported the development and operation of the Optical Transient Detector (the *MicroLab 1* satellite's primary experiment) and 1-Hz tracking stations needed for GPS/MET as part of the International GPS Service network. Orbital Sciences Corporation accommodated the GPS/MET payload on its Microlab satellite and provided a Pegasus rocket launch. Allen Osborne Associates, Inc. worked with GPS/MET investigators to convert its commercial TurboRogue GPS receiver for use in space. Part of the work was supported by the Independent Research program of Lockheed Martin Missiles and Space.

References

Ahnert, P. R., 1991: Precision and comparability of National Weather Service upper air measurements. Preprints, *Seventh Symp. on Meteorological Observations and Instruments,* New Orleans, LA, Amer. Meteor. Soc., 221–226.

Bengtsson, L., M. E. Gorbunov, and S. V. Sokolovskiy, 1995: Space refractive tomography of the atmosphere: Modeling of direct and inverse problems. Max–Planck–Institute for Meteorology Tech. Rep., Hamburg, Germany, in press.

Bevis, M., S. Businger, T. A. Herring, C. Rocken, R. A. Anthes, and R. H. Ware, 1992: GPS meteorology: Remote sensing of atmospheric water vapor using the global positioning system. *J. Geophys. Res.,* **97**(D14), 15 787–15 801.

Brewster, K. A., S. T. Benjamin, and R. Crawford, 1989: Quality control of ACARS meteorological observations—a preliminary data survey. Preprints, *Third Int. Conf. on Aviation Weather Systems,* Anaheim, CA, Amer. Meteor. Soc., 124–129.

Businger, S., S. R. Chiswell, M. Bevis, J. Duan, R. A. Anthes, C. Rocken, R. Ware, T. Van Hove, and F. Solheim, 1996: The promise of GPS in atmospheric monitoring. *Bull. Amer. Meteor. Soc.,* **77,** xxxx–xxxx pp.

Dalaudier, F., A. S. Gurvich, V. Kan, and C. Sidi, 1994: Middle stratosphere temperature spectra observed with stellar scintillations and in situ techniques. *Adv. Space Res.,* **14,** 961–964.

Elliot, W. P., and D. J. Gaffen, 1991: On the utility of radiosonde humidity archives for climate studies. *Bull. Amer. Meteor. Soc.,* **72,** 1507–1520.

Eyre, J. R., 1994: Assimilation of radio occultation measurements into a numerical weather prediction system. ECMWF Tech. Memo. 199, 34 pp.

Fjeldbo, G., and V. R. Eshleman, 1968: The atmosphere of Mars analyzed by integral inversion of the Mariner IV occultation data. *Planet. Space Sci.,* **16,** 123–140.

——, and ——, 1969: Atmosphere of Venus as studied with the Mariner V dual radio-frequency occultation experiment. *Radio Sci.,* **4,** 879–897.

——, A. J. Kliore, and V. L. Eshleman, 1971: The neutral atmosphere of Venus as studied with the Mariner V radio occultation experiments. *Astron. J.,* **76,** 123–140.

Gaffen, D. J., W. P. Elliott, and A. Robock, 1992: Relationships between tropospheric water vapor and surface temperature as observed by radiosondes. *Geophys. Res. Lett.,* **19,** 1839–1842.

Gorbunov, M. E., and S. V. Sokolovskiy, 1993: Remote sensing of refractivity from space for global observations of atmospheric parameters. Max–Planck–Institute for Meteorology Rep. 119, Hamburg, Germany, 58 pp.

Gurvich, A. S., V. Kan, L. I. Popov, V. V. Ryumin, S. A. Savchenko, and S. V. Sokolovskiy, 1982: Reconstruction of the atmosphere's temperature profile from motion pictures of the sun and moon taken from the "Salyut-6" orbiter. *Izv. Atmos. Oceanic Phys.,* **18,** 1–4.

Hajj, G. A., and E. R. Kursinski, 1991: Analysis of errors in the vertical temperature profiles recovered from GPS occultation observations. *Trans. Amer. Geophys. Union,* **72,** 372.

——, ——, W. L. Bertiger, L. J. Romans, and K. R. Hardy, 1994: Assessment of GPS occultations for atmospheric profiling. Preprints, *Seventh Conf. on Satellite Meteorology and Oceanography,* Monterey, CA, Amer. Meteor. Soc., J7–J10.

Hardy, K. R., D. P. Hinson, G. L. Tyler, and E. R. Kursinski, 1992: Atmospheric profiles from active space-based radio measurements. Preprints, *Sixth Conf. on Satellite Meteorology and Oceanography,* Atlanta, GA, Amer. Meteor. Soc., 420–423.

——, G. A. Hajj, and E. R. Kursinski, 1993: Accuracies of atmospheric profiles obtained from GPS occultations. *Proc. Institute of Navigation GPS-'93 Conf.,* Salt Lake City, UT, Institute of Navigation, 1545–1556.

Hayden, C. M., 1988: GOES-VAS simultaneous temperature–moisture retrieval algorithm. *J. Appl. Meteor.,* **27,** 705–733.

Houghton, J. T., G. J. Jenkins, and J. J. Ephraums, Eds., 1990: *Scientific Assessment of Climate Change.* Cambridge University Press, 365 pp.

——, B. A. Callander, and S. K. Varney, Eds., 1992: *Climate Change 1992.* Cambridge University Press, 200 pp.

Hurrell, J. W., and K. E. Trenberth, 1992: An evaluation on monthly mean MSU and ECMWF global atmospheric temperatures for monitoring climate. *J. Climate,* **5,** 1424–1440.

Illari, L., 1989: The quality of satellite precipitable water content data and their impact on analyzed moisture fields. *Tellus,* **41A,** 319–337.

Kliore, A. J., D. L. Cain, G. S. Levy, V. R. Eshlemann, G. Fjeldbo, and F. D. Drake, 1965: Occultation experiment: Results of the first direct measurement of Mars' atmosphere and ionosphere. *Science,* **149,** 1243–1248.

——, G. Fjeldbo, B. L. Seidel, D. N. Seetnam, T. T. Sesplaukis, P. M. Woiceshyn, and S. I. Rasool, 1975: The atmosphere of Io from Pioneer 10 radio occultation measurements. *Icarus,* **24,** 407–410.

Kursinski, E. R., G. A. Hajj, and K. R. Hardy, 1993: Temperature or moisture profiles from radio occultation measurements. Preprints, *Eighth Symp. on Meteorological Observation and Instrumentation,* Anaheim, CA, Amer. Meteor. Soc., J153–J158.

Lee, H. S., and F. J. Schmidlin, 1991: Comparisons of satellite-retrieved layer temperature and correlative radiosonde data. Preprints, *Seventh Symp. on Meteorological Observations and Instruments,* New Orleans, LA, Amer. Meteor. Soc., 276–280.

Lindal, G. F., 1992: The atmosphere of Neptune: An analysis of radio occultation data acquired with voyager. *Astron. J.,* **103,** 967–982.

——, H. B. Hotz, D. N. Sweetnam, Z. Shippony, J. P. Brenkle, G. V. Hartsell, R. T. Spear, and W. H. Michael, 1979: Viking radio occultation measurements of the atmosphere and topography of Mars: Data acquired during 1 Martian year of tracking. *J. Geophys. Res.,* **84,** 8443–8456.

——, and Coauthors, 1981: The atmosphere of Jupiter: An analysis of the Voyager radio occultation measurements. *J. Geophys. Res.,* **86,** 8721–8727.

——, G. E. Wood, H. B. Hotz, D. N. Sweetnam, V. R. Eshleman, and G. L. Tyler, 1983: The atmosphere of Titan: An analysis of the Voyager 1 radio occultation measurements. *Icarus,* **53,** 348–363.

——, D. N. Sweetnam, and V. R. Eshleman, 1985: The atmosphere of Saturn: An analysis of the Voyager radio occultation measurements. *Astron. J.,* **90,** 1136–1146.

——, J. R. Lyons, D. N. Sweetnam, V. R. Eshleman, D. P. Hinson, and G. L. Tyler, 1987: The atmosphere of Uranus: Results of radio occultation measurements with Voyager 2. *J. Geophys. Res.,* **92,** 14 987–15 001.

——, ——, ——, ——, ——, and ——, 1990: The atmosphere of Neptune: Results of radio occultation measurements with the Voyager 2 spacecraft. *Geophys. Res. Lett.,* **17,** 1733–1736.

Luers, J. K., and R. E. Eskridge, 1995: Temperature corrections for the VIZ and Vaisala radiosondes. *J. Appl. Meteor.,* **34,** 1241–1253.

Malla, R. P., S. C. Wu, and S. M. Lichten, 1992: Geocenter location and variations in Earth orientation using GPS. *J. Geophys. Res. (Solid Earth),* **98,** 4611–4617.

Meehan, T. K., E. R. Kursinski, G. A. Hajj, J. M. Srinivasan, and S. J. DiNardo, 1991: Analysis of GPS signals occulted by the atmosphere as tracked from Mauna Kea using the TurboRogue GPS receiver. *Trans. Amer. Geophys. Union,* **72,** 372.

Melbourne, W. G., T. P. Yunck, L. E. Young, B. H. Hager, G. F. Lindal, C. H. Liu, and G. H. Born, 1988: GPS geoscience instrument for EOS and Space Station. JPL Proposal to NASA AO OSSA-1-88, 81 pp.

——, and Coauthors, 1994a: The application of spaceborne GPS to atmospheric limb sounding and global change monitoring. JPL Publ. 94-18, 147 pp.

——, B. D. Tapley, and T. P. Yunck, 1994b: The GPS flight experiment on TOPEX/POSEIDON. *Geophys. Res. Lett,* **21,** 2171–2174.

Nash, J., and F. J. Schmidlin, 1987: WMO international radiosonde comparison, instruments and observing methods. World Meteorological Organization Rep. 30, WMO/TD-No. 195, 103 pp.

Newman, M., G. Schubert, A. J. Kliore, and I. R. Patel, 1984: Zonal winds in the middle atmosphere of Venus from Pioneer Venus radio occultation data. *J. Atmos. Sci.,* **41,** 1901–1913.

NOAA, 1992: *Strategic Plan for Upper Air Observations.* 18 pp.

Phinney, R. A., and D. L. Anderson, 1968: On the radio occultation method for studying planetary atmospheres. *J. Geophys. Res.,* **73,** 1819–1827.

Rind, D., E.-W. Chiou, W. Chu, J. Larsen, S. Oltmans, J. Lerner, M. P. McCormick, and L. McMaster, 1991: Positive water vapor feedback in climate models confirmed by satellite data. *Nature,* **349,** 500–503.

Rocken, C., and C. Meertens, 1991: Monitoring selective availability dither frequencies and their effect on GPS data. *Bull. Geodesique,* **71,** 162–169.

Schlussel, P., and W. J. Emery, 1990: Atmospheric water vapor over the oceans from SSM/I measurements. *Int. J. Remote Sens.,* **11,** 753–766.

Schwartz, B. E., and C. A. Doswell, 1991: North American rawinsonde observations: Problems, concerns, and a call to action. *Bull. Amer. Meteor. Soc.,* **72,** 1885–1896.

Shea, D. J., S. J. Wifley, I. R. Stern, and T. J. Hoar, 1994: An introduction to atmospheric and oceanographic data. NCAR Tech. Note NCAR/TN-4044 IA, 132 pp.

Smith, W. L., and Coauthors, 1990: GHIS—The GOES High-Resolution Interferometer Sounder. *J. Appl. Meteor.,* **29,** 1189–1204.

Spencer, R. W., and J. R. Christy, 1990: Precise monitoring of global temperature trends from satellites. *Science,* **247,** 1558–1562.

——, ——, and N. C. Grody, 1990: Global atmospheric temperature monitoring with satellite microwave measurements: Method and results 1979–84. *J. Climate,* **3,** 1111–1128.

Spilker, J. J., 1978: GPS signal structure and performance characteristics. *J. Inst. Nav.,* **25**(2), 121–146.

Trenberth, K. E., 1995: Atmospheric circulation climate changes. *Clim. Change,* **31,** 427–453.

——, J. R. Christy, and J. W. Hurrell, 1992: Monitoring global monthly mean surface temperatures. *J. Climate,* **5,** 1405–1423.

Tyler, G. L., 1987: Radio propagation experiments in the outer solar system with Voyager. *Proc. IEEE,* **75,** 1404–1431.

——, and Coauthors, 1989: Voyager radio science observations of Neptune and Triton. *Science,* **246,** 1466–1473.

Van Loon, H., and K. Labitzke, 1990: Association between the 11-year solar cycle and the atmosphere. Part IV: The stratosphere, not grouped by the phase of the QBO. *J. Climate,* **3,** 827–837.

Vorob'ev, V. V., and T. G. Krasilnikova, 1994: Estimation of the accuracy of the atmospheric refractive index recovery from Doppler shift measurements at frequencies used in the NAVSTAR system. *Phys. Atmos. Ocean,* **29,** 602–609.

Ware, R., 1992: GPS sounding of Earth's atmosphere. *GPS World,* **3,** 56–57.

——, and S. Businger, 1995: Global positioning finds applications for geosciences research. *Trans. Amer. Geophys. Union,* **76,** 187.

——, M. Exner, B. Herman, W. Kuo, and T. Meehan, 1993: Active atmospheric limb sounding with an orbiting GPS receiver. *Trans. Amer. Geophys. Union,* **74,** 336.

Yuan, L., R. A. Anthes, R. H. Ware, C. Rocken, W. Bonner, M. Bevis, and S. Businger, 1993: Sensing climate change using the global positioning system. *J. Geophys. Res.,* **98**(D8), 14 925–14 937.

Zou, X., Y.-H. Kuo, and Y.-R. Guo, 1995: Assimilation of atmospheric radio refractivity using a nonhydrostatic mesoscale model. *Mon. Wea. Rev.,* **123,** 2229–2249.

Zumberge, J., R. Neilan, G. Beutler, and J. Kouba, 1994: The international GPS service for geodynamics-benefits to users. *Proc. Seventh Technical Meeting of the Institute of Navigation,* Institute of Navigation, Salt Lake City, UT, 1663–1666

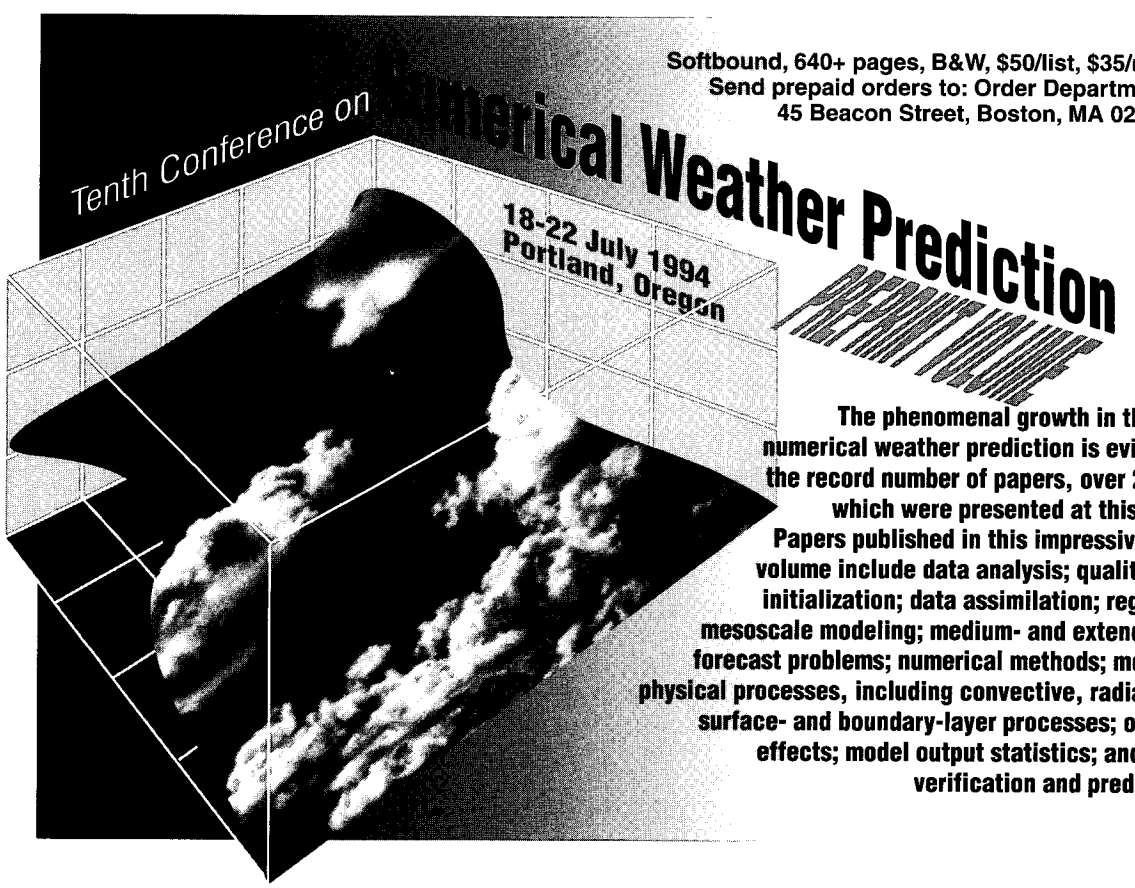

Softbound, 640+ pages, B&W, $50/list, $35/members. Send prepaid orders to: Order Department, AMS, 45 Beacon Street, Boston, MA 02108-3693.

The phenomenal growth in the field of numerical weather prediction is evident from the record number of papers, over 285 in all, which were presented at this meeting. Papers published in this impressive preprint volume include data analysis; quality control; initialization; data assimilation; regional and mesoscale modeling; medium- and extended-range forecast problems; numerical methods; modeling of physical processes, including convective, radiative, and surface- and boundary-layer processes; orographic effects; model output statistics; and forecast verification and predictability.

The Promise of GPS in Atmospheric Monitoring

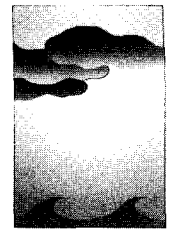

Steven Businger,* Steven R. Chiswell,* Michael Bevis,* Jingping Duan,*
Richard A. Anthes,+ Christian Rocken,# Randolph H. Ware,#
Michael Exner,# T. VanHove,# and Fredrick S. Solheim#

ABSTRACT

This paper provides an overview of applications of the Global Positioning System (GPS) for active measurement of the Earth's atmosphere. Microwave radio signals transmitted by GPS satellites are delayed (refracted) by the atmosphere as they propagate to Earth-based GPS receivers or GPS receivers carried on low Earth orbit satellites.

The delay in GPS signals reaching Earth-based receivers due to the presence of water vapor is nearly proportional to the quantity of water vapor integrated along the signal path. Measurement of atmospheric water vapor by Earth-based GPS receivers was demonstrated during the GPS/STORM field project to be comparable and in some respects superior to measurements by ground-based water vapor radiometers. Increased spatial and temporal resolution of the water vapor distribution provided by the GPS/STORM network proved useful in monitoring the moisture-flux convergence along a dryline and the decrease in integrated water vapor associated with the passage of a midtropospheric cold front, both of which triggered severe weather over the area during the course of the experiment.

Given the rapid growth in regional networks of continuously operating Earth-based GPS receivers currently being implemented, an opportunity exists to observe the distribution of water vapor with increased spatial and temporal coverage, which could prove valuable in a range of operational and research applications in the atmospheric sciences.

The first space-based GPS receiver designed for sensing the Earth's atmosphere was launched in April 1995. Phase measurements of GPS signals as they are occluded by the atmosphere provide refractivity profiles (see the companion article by Ware et al. on page 19 of this issue). Water vapor limits the accuracy of temperature recovery below the tropopause because of uncertainty in the water vapor distribution. The sensitivity of atmospheric refractivity to water vapor pressure, however, means that refractivity profiles can in principle yield information on the atmospheric humidity distribution given independent information on the temperature and pressure distribution from NWP models or independent observational data.

A discussion is provided of some of the research opportunities that exist to capitalize on the complementary nature of the methods of active atmospheric monitoring by GPS and other observation systems for use in weather and climate studies and in numerical weather prediction models.

1. Introduction

Soon after the launch of the space age, it was recognized that the predictable orbits of satellites provide a valuable reference frame for global navigation systems. Twenty years ago, the first Global Positioning System (GPS) tracking network was established by the U.S. military to link the satellite reference frame to Earth. The military network includes five globally distributed tracking stations that provide orbit determinations with 10-m accuracy. More recently, civilian organizations from various nations have established the International GPS Service network, which includes more than 50 globally distributed tracking stations and provides orbit determination with 50-cm accuracy in support of geodetic and geophysical research activities.

*Department of Meteorology, University of Hawaii, Honolulu, Hawaii.
+University Corporation for Atmospheric Research, Boulder, Colorado.
#University Navstar Consortium (UNAVCO), Boulder, Colorado.
Corresponding author address: Steven Businger, Dept. of Meteorology, University of Hawaii, 2525 Correa Road, Honolulu, HI 96822.
In final form 25 September 1995.
©1996 American Meteorological Society

Today, the Global Positioning System consists of a constellation of 24 satellites that transmit L-band radio signals (~19- and 22-cm wavelengths) to large numbers of users engaged in navigation, time transfer, and relative positioning. A number of applications of meteorological utility have emerged as a product of this positioning technology. For example, as the cost and weight of GPS receivers have decreased, they are increasingly being used in balloon instrument transponders to provide location information and, thereby, information on layer-mean winds. There is also the possibility of using the receivers for quasi-Lagrangian air parcel tracking (e.g., Businger et al. 1996; Barat and Cot 1995). GPS technology can provide wind speed measurements with an accuracy of 0.1 m s^{-1}, is not susceptible to atmospheric electrical interference, and allows for simultaneous tracking of multiple balloons. These advantages, in addition to threats of the demise of the navigational aids loran (Long Range Navigation) and Omega, favor GPS systems for radiosonde and dropwindsonde applications (e.g., Boire et al. 1993). Accurate position and timing information is also crucial to research that uses the travel time of acoustic waves to probe global sea surface temperatures; the travel time of acoustic waves can then be related to the mean sea surface temperature along the path of the wave. This paper will focus on the application of GPS in active atmospheric measurement.

There are two primary methods by which GPS can be used to actively sense properties of the Earth's atmosphere. The first technique involves data collected by dual-frequency GPS receivers at fixed locations on the ground. GPS signals are delayed and refracted by the gases composing the atmosphere as they propagate from GPS satellites to the Earth-based receivers (Fig. 1). In particular, a significant and unique delay is introduced by water vapor because it is the only common atmospheric constituent that possesses a permanent dipole moment. This dipole moment is caused by an asymmetric distribution of charge in the water molecule, and it retards the propagation of electromagnetic radiation through the atmosphere. Per mole, the refractivity of water vapor is ~17 times that of dry air. Water's permanent dipole moment is also directly responsible for the unusually large latent energy associated with water's changes of phase, which in turn significantly impacts the vertical stability of the atmosphere, the structure and evolution of storm systems, and the meridional and radiational energy balance of the earth–atmosphere system. Thus, knowledge of the distribution of water vapor is essential in understanding weather and global climate (Stephens and Greenwald 1991; IPCC 1992).

The sensitivity of atmospheric refractivity to the presence of water vapor makes it possible for Earth-based GPS receivers to provide time series data on integrated water vapor above the receiver site. The delay in propagation of microwave radiation to Earth-based receivers introduced by water vapor is referred to as the "wet delay" and is nearly proportional to the quantity of vapor integrated along the signal path. In liquid water and ice, the hydrogen bond between water molecules greatly reduces the contribution of the dipole moment to the delay. Thus, the presence of cloud water and ice does not discernibly affect the GPS measurement of water vapor. The ionospheric delay is dispersive (frequency dependent) and can be determined by observing both of the frequencies transmitted by GPS satellites and exploiting the known dispersion relations for the ionosphere (Spilker 1980; Brunner and Gu 1991). Ionospheric delays affecting observations recorded by a dual-frequency GPS receiver can be eliminated without reference to observations recorded by other GPS receivers in the same network. If the position of the receiver is accurately known and the ionospheric delay has been accounted for, an estimate of the vertically integrated water vapor overlying the receiver can be derived from the GPS signals and observations of surface temperature and pressure (Bevis et al. 1992, 1994; Rocken et al. 1993, 1995; Duan et al. 1996). Integrated water vapor represents the total latent heat available in the column from the vapor, and as such it has the potential to provide a powerful constraint to numerical weather prediction (NWP) models (Kuo et al. 1993, 1996) and in weather analysis.

A second approach for monitoring the Earth's atmosphere using GPS signals arises from efforts more than 30 years ago to study the atmospheres of other planets (see Melbourne et al. 1994 for a review). Coherent dual-band radio signals transmitted by a radio telescope to a spacecraft on the far side of a planet are bent through the planet's atmosphere on their way back to Earth, where a receiver picks up the signal. Profiles of the planetary atmosphere's pressure and temperature are then recovered from the two-way differential phase measurements (Melbourne 1976). Radio occultation, as this technique is called, has been used to probe the atmospheres and ionospheres of the planets and their moons, as well as certain physical properties of planetary surfaces and planetary rings (e.g., Fjeldbo et al. 1971; Lindal et al. 1981).

With the recent launch of a GPS receiver on a low Earth orbit (LEO) satellite (see the companion article by Ware et al. 1996), the radio occultation technique is now being applied to the Earth's atmosphere. When the GPS receiver aboard the LEO tracks a GPS satellite as it occults the Earth's atmosphere, the arrival time of the GPS signal at the receiver is delayed because of the refractive bending and slowing of the signal as it traverses the atmosphere (Fig. 1). By measuring the change in carrier phase over the entire occultation event (~60 s for the neutral atmosphere), the atmospheric refractive index can be determined as a function of altitude. Temperature and pressure profiles can then be derived through a downward integration using the known linear relationship between refractivity and density of dry air, the gas law, and the assumption of hydrostatic equilibrium.

Water vapor, the most variable and inhomogeneous of the major constituents of the troposphere, limits the accuracy of temperature recovery below the tropopause because of uncertainty in the water vapor distribution. However, the sensitivity of atmospheric refractivity to water vapor pressure means that refractivity profiles can in principle yield information on the global atmospheric humidity distribution and abundance, given independent information on the temperature and pressure distribution from NWP models or independent observational data (Gurvich and Krasil'nikova 1990; Gorbunov and Sokolovskiy 1993; Ware et al. 1996).

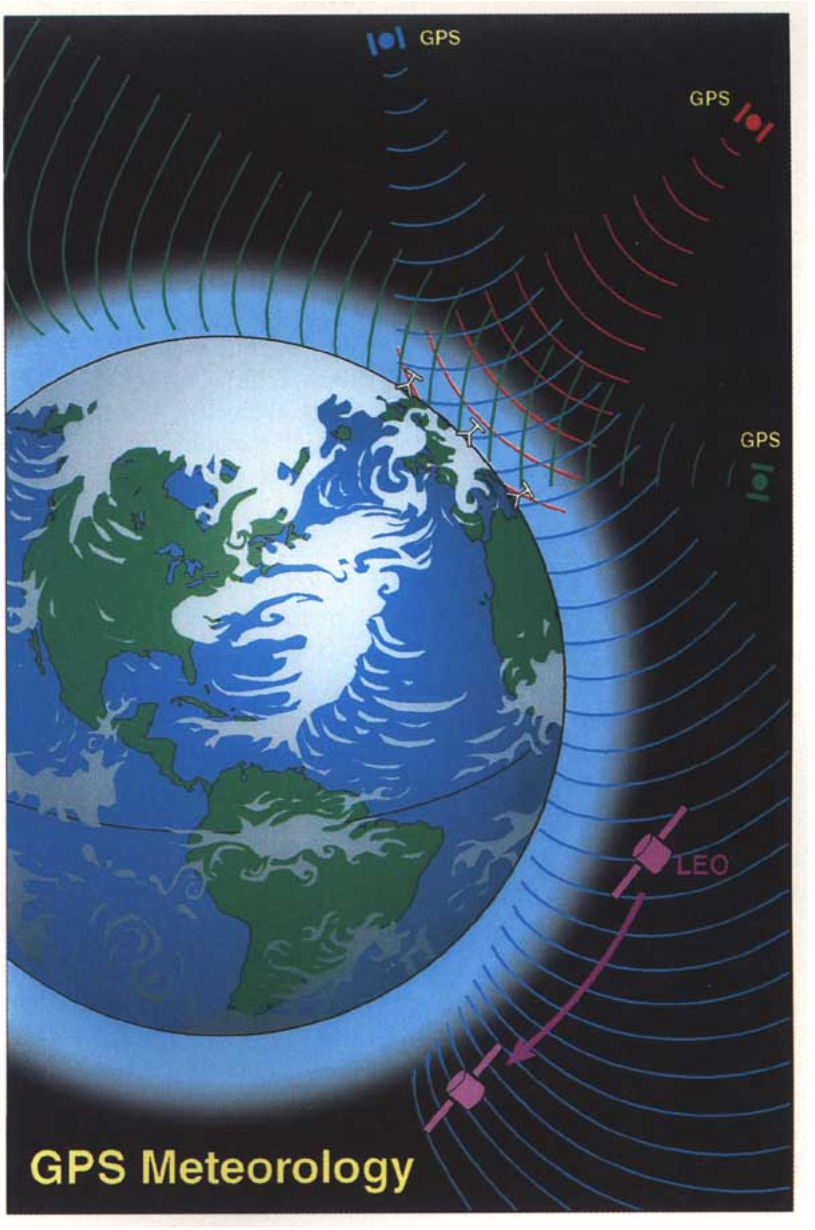

FIG. 1. A schematic diagram of GPS meteorology showing GPS signals passing from GPS satellites, orbiting at heights of ~20 000 km, through the intervening Earth's atmosphere to Earth-based receivers and to a low Earth orbit satellite. The delay of signals arriving at Earth-based receivers is proportional to the intervening integrated water vapor. Signals propagating from the GPS satellite to the LEO satellite at a height of about 775 km are refracted by the Earth's atmosphere during the ~60-s period before the signal is occulted by the Earth, providing a refractivity profile of the atmosphere.

2. Earth-based GPS meteorology: A meteorological signal from geodetic noise

A primary task of geodetic GPS algorithms is to calibrate the delay or "equivalent excess path length" introduced by the refractivity of the Earth's atmosphere. The ionosphere introduces a delay that can be determined and removed by recording the phase angles of the carriers of both of the frequencies transmitted by GPS satellites and exploiting known dispersion relations for the ionosphere (Spilker 1980). The remaining delay, due to the electrically neutral atmosphere, can be divided into two parts: a *hydrostatic*

delay and a *wet delay* (Saastamoinen 1972; Davis et al. 1985). Both delays are smallest for paths oriented along the zenith direction and increase approximately inversely with the sine of the elevation angle. Most expressions for the delay along a path of arbitrary elevation consist of the zenith delay multiplied by a *mapping function* that describes the dependence on elevation angle (Davis et al. 1985; Leick 1990). For example, assuming the atmosphere above a GPS antenna is azimuthally isotropic and neglecting the curvature of the Earth, the wet delay along a line with elevation angle e is related to the zenith wet delay by the mapping function $(\sin e)^{-1}$: wet delay equals zenith wet delay times $(\sin e)^{-1}$, where e is the elevation angle.

Since the hydrostatic delay is due to the transient or induced dipole moment of all the gaseous constituents of the atmosphere including water vapor, the term hydrostatic delay is favored over the sometimes used term "dry delay." The hydrostatic delay is well determined from pressure measurements, and at sea level it typically reaches about 2.3 m in the zenith direction. It is possible to calculate the zenith hydrostatic delay to better than 1 mm, given surface pressure measurements accurate to 0.3 mb or better. The basis for estimating the precipitable water in the atmosphere arises from the fact that the wet delay is closely related to the quantity of water vapor overlying the receiver. The zenith wet delay (ZWD) can be less than 10 mm in arid regions and as large as 400 mm in humid regions. Significantly, the daily variability of the wet delay usually exceeds that of the hydrostatic delay by more than an order of magnitude, especially in temperate areas (e.g., Elgered et al. 1990). Zenith wet delay can be estimated from GPS data as part of the overall least squares inversion for the coordinates of the GPS receivers, the orbital parameters of the GPS satellites, and other geodetic parameters of interest (Bevis et al. 1992; Rocken et al. 1993; Duan et al. 1996).

If we state integrated water vapor in terms of precipitable water (PW), the height of an equivalent column of liquid water is

$$\mathrm{PW} = \int_0^\infty r \frac{\rho_a}{\rho_w} dz, \tag{1}$$

where r is the mixing ratio, ρ_a is the density of dry air, and ρ_w is the density of liquid water. It can then be shown (Askne and Nordius 1987; Bevis et al. 1994) that

$$\mathrm{PW} = \Pi(\mathrm{ZWD}), \tag{2}$$

where ZWD is given in units of length. The dimensionless *constant* of proportionality

$$\Pi = 10^6 \left[\rho_w R_v \left(k_3 / T_m + k_2' \right) \right]^{-1} \tag{3}$$

is a function of empirical constants related to the refractivity of moist air (k_3 *and* k_2'), the gas constant for water vapor (R_v), and a *mean temperature* of the atmosphere T_m defined (Davis et al. 1985) as

$$T_m = \frac{\int (e/T) dz}{\int (e/T^2) dz}, \tag{4}$$

where e is the water vapor pressure and T is the temperature.

As a rough rule of thumb, the ratio PW/ZWD = Π ~ 0.15, but the actual value of the parameter Π depends on the summation of the local climate controls (e.g., location, elevation, and season) and it can vary by as much as 15% (Bevis et al. 1992). Figure 2 shows the daily and seasonal variability in Π calculated from radiosonde data for Greensboro, North Carolina. It is significant that the amplitude of the daily fluctuations is of the same order of magnitude as that of the seasonal change. Nearly all of the spatial and temporal variability of Π is derived from the variability of T_m. Therefore, the accuracy with which a GPS-derived

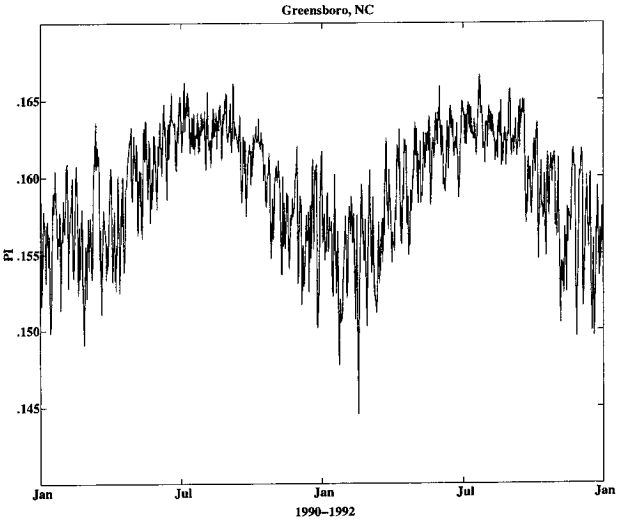

FIG. 2. Ratio of PW to ZWD, or Π, calculated for two years (January 1990 to January 1992) of radiosonde data from Greensboro, North Carolina.

ZWD estimate can be transformed into an estimate of PW is determined by the accuracy to which we can estimate the value of T_m. By using NWP models to estimate T_m at each GPS receiver as a function of time, one can estimate the coefficient Π used to map the ZWD onto PW with a relative error of less than ±1% (Bevis et al. 1994). Alternatively, in an approach that is more convenient but slightly less accurate (±2%), one can use a regression based on surface temperature and climatology (Bevis et al. 1992). Rocken et al. (1993) and Bevis et al. (1994) provide more comprehensive discussions of error sources.

Most GPS processing software packages in use today model the neutral atmospheric delay given the assumption of azimuthal isotropy. That is, mapping functions characterize line of sight (or *pointed*) delays solely in terms of the zenith delay and elevation angle measured from a *horizon* 90° from the local zenith. In fact, horizontal refractivity gradients, mainly associated with the inhomogeneity of water vapor, are known to produce azimuthal variations in delay (Ware et al. 1996). Algorithms have been developed to characterize azimuthal anisotropy (Herring 1992). To do so, it is necessary to increase the number of parameters from one (the zenith delay) to at least three and the number of predictor variables from one (elevation) to two (elevation and azimuth). The estimation of azimuthal variation is currently used in Very Long Baseline Interferometry analysis, and it is likely that this new class of mapping function will be incorporated in GPS processing on a routine basis. The advantages are twofold: taking proper account of azimuthal anisotropy will lead to better estimates of the zenith wet delay and, hence, PW, and information will be provided on the direction and magnitude of horizontal gradients in PW.

3. Results from the field

During May 1993, a field experiment called GPS/STORM was conducted to evaluate Earth-based GPS measurement of atmospheric water vapor in a region infamous for severe weather. During GPS/STORM, university and UNAVCO[1] scientists installed GPS receivers and ground-based microwave radiometers at five National Oceanic and Atmospheric Administration (NOAA) wind profiler sites and at the Department of Energy's (DOE) Southern Great Plains Cloud and Radiation Testbed sites near Lamont (LAMO), Oklahoma (Fig. 3, top).[2] The sites were chosen to take advantage of the existing operational infrastructure at the NOAA profiler sites. The mounted GPS receiver antenna is shown in Fig. 4.

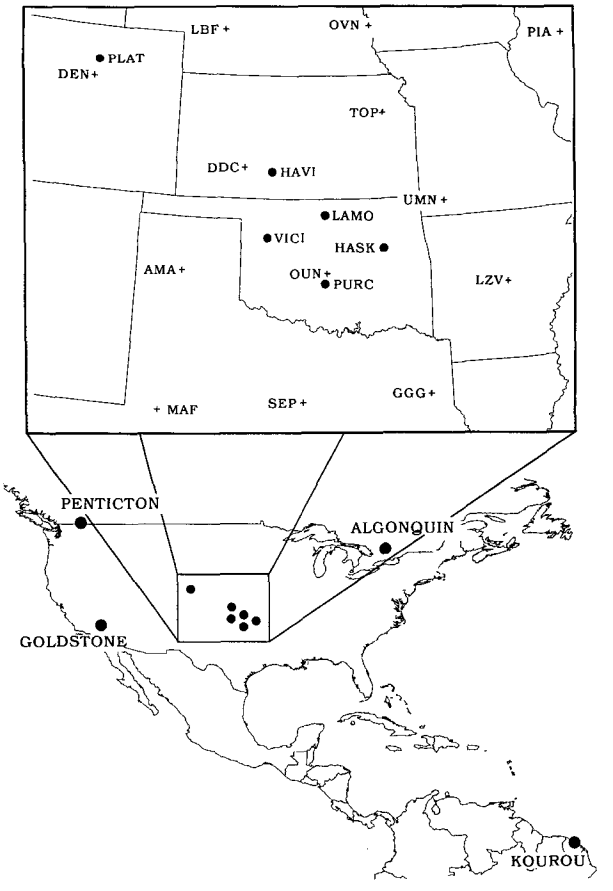

FIG. 3. (Top) Map of the GPS/STORM region showing the locations of the GPS receivers (•) and NWS radiosonde sites (+). (Bottom) Map showing remote GPS sites (labeled circles) used in absolute water vapor estimation.

To estimate the zenith wet delay (ZWD) and thus PW, knowledge of the station position and the satellite orbits is required. Precise orbits were obtained via the Internet from the International GPS Service (Zumberge et al. 1994) and from the Scripps Orbit and Permanent Array Center (SOPAC). During the field experiment, five or more satellites were typically

[1]The University Navstar Consortium (UNAVCO) provides equipment and assistance to academic investigators using GPS for scientific research. UNAVCO operates as a program of the University Corporation for Atmospheric Research and is supported by the National Science Foundation and NASA.

[2]GPS/STORM was funded by the National Science Foundation and was conducted in coordination with NOAA's Forecast Systems Laboratory Demonstration Division and the DOE Atmospheric Radiation Measurement program.

FIG. 4. Photograph of a GPS receiver antenna mounted on the perimeter fence of a NOAA wind profiler. The diameter of the antenna ground plane shown is ~50 cm.

visible at any time at each receiver site. For GPS networks with a separation between receivers of less than ~500 km, both the deterministic (least squares) and Kalman filtering techniques used to estimate zenith delay are more sensitive to relative rather than absolute delays (Rocken et al. 1993, 1995). This is because a GPS satellite observed by two or more receivers is viewed at almost identical elevation angles, causing the delay estimates to be highly correlated. Therefore, the estimates of ZWD derived from a small network are subject to an unknown bias for each sampling period. The value of the bias is constant across the whole network (i.e., the bias varies in time but not in space). One approach to estimating this bias is to measure PW with a ground-based water vapor radiometer (radiometer, hereafter) at a single reference site and use the GPS data to estimate PW relative to this reference site at any number of so-called secondary sites in the monitoring network. This procedure is known as *levering*. (One levers the group of biased PW estimates until they all have the correct absolute value.) Rocken et al. (1995) show PW results using radiometer levering and find an rms error of ~1.5 mm and a bias of <0.5 mm when comparing PW from GPS receivers with that from radiometers.

An attractive alternate approach that eliminates the need for an independent measurement of PW at a reference site is to add a few outlying GPS stations to the receiver network that introduce baselines much longer than 500 km (e.g., Fig. 3). Provided GPS satellite orbit information of sufficient accuracy (~50 cm) is available, it is possible to estimate absolute ZWD and, therefore, absolute PW from the GPS observations alone. Rocken et al. (1995) noted that the difference, or error, between absolute PW estimation derived solely from GPS/STORM GPS data and that derived from radiometers was about 15% greater than the error when comparing radiometer-levered PW results with the radiometer PW values. Duan et al. (1996) included outlying GPS reference sites in Canada, California, and French Guiana (Fig. 3, bottom) and found errors slightly smaller than those obtained with radiometer levering. A complete description of the absolute estimation technique is given in Duan et al. (1996), which is the source of the GPS PW data in this paper. The radiometer data are from Rocken et al. (1995).

Subsequently, the NOAA's Environmental Research Laboratories, in an effort to implement the capability to monitor atmospheric water vapor in real time using GPS signal delay within NOAA, has coordinated a comprehensive comparison of GPS-derived PW data with radiometer PW data (NOAA 1995). The results of the tests show that when compared with rawinsonde observation, GPS-derived PW estimates are comparable in accuracy and precision to radiometer estimates. The reader is referred to the NOAA (1995) document for details of the statistics.

From a logistical perspective, the weather during GPS/STORM proved a major challenge. Hardware sustained considerable damage due to lightning strikes, including the loss of six personal computers used in data logging. However, GPS receivers escaped harm. During the period 6–9 May 1993, over 100 tornadoes, including an F-4 intensity tornado over Kansas, were reported in the general area of the field experiment, accompanying a slow-moving dryline. Previous research has documented the association of severe weather with such features (Schaefer 1974; McCarthy and Koch 1982; Parsons et al. 1991).

GPS-derived PW data from this period show fluctuations associated with the diurnal shift of the dryline

back and forth across the network (Fig. 5). Superimposed on the more gradual changes in PW associated with the changing position of the dryline are rapid changes in PW that appear in many cases to precede thunderstorm development (Fig. 5). These increases are consistent with moisture flux convergence, which has long been recognized as essential to convection (e.g., Kuo 1965). Charba (1979) found this quantity second only to the Modified Total–Totals index as a model output statistics predictor of local severe weather. Case studies (e.g., Waldstreicher 1989; Businger et al. 1991) have shown that storms often form in areas where moisture flux convergence is increasing rapidly with time and where the gradient in moisture flux convergence is tightening. Time series GPS PW data by themselves do not allow the forecaster to discriminate between advection and locate time-rate-of-change increases in PW at a single receiver site. However, in combination with other data sources, such as Doppler radar and satellites, the GPS PW time series have the potential to be valuable in short-term forecasting applications.

The scale of weather features that future GPS networks will be able to resolve spatially will depend in part upon the distance between receivers in the network. Figure 6 illustrates the impact of GPS PW data from five receiver sites on a synoptic objective analysis in the GPS/STORM region. Since moisture in this case was confined to the lower troposphere by a shallow capping inversion, the location of the dryline provides a qualitative reference for the accuracy of the analysis. The analysis using only radiosonde data shows relatively dry air over western Oklahoma (Fig. 6a), in conflict with the GPS data and in conflict with the analyzed position of the dryline shown in Fig. 6b. Qualitatively, the best agreement between the position of the dryline and the analysis of PW occurs in the heart of the GPS network, where the greatest concentration of supplemental data resides. The high PW value (32 mm) at Vici, Oklahoma, (VICI) is consistent with thunderstorm activity observed in that area and illustrates the degree of local variability in the distribution of atmospheric water vapor.

During the period 23–24 May 1993, midtropospheric advection of relatively cold, dry air triggered convection and was associated with numerous reports of large hail and damaging winds in southern Oklahoma and northern Texas and several reports of funnel clouds or tornadoes in north Texas. Intrusions of cold, dry air at midlevels ahead of surface cold fronts or drylines have been described as cold fronts aloft (CFA) (Locatelli et al. 1989; Hobbs et al. 1990; Businger et al. 1991) and are not detected in standard surface observations. Figure 7 shows the drop in integrated water vapor at Purcell, Oklahoma, prior to the arrival of the surface front, illustrating the signature of this feature in the PW data. The advance of the cold front aloft across the surface cold front was a primary factor in the initiation of severe weather over the GPS/STORM region, because it generated convective instability and entrained dry air into thunderstorm downdrafts (Chiswell et al. 1996).

The temporal resolving power represented by the GPS data is demonstrated when a comparison is made between time series cross sections of equivalent potential temperature with and without the GPS PW data (Fig. 8). Combining radiosonde and GPS PW data can

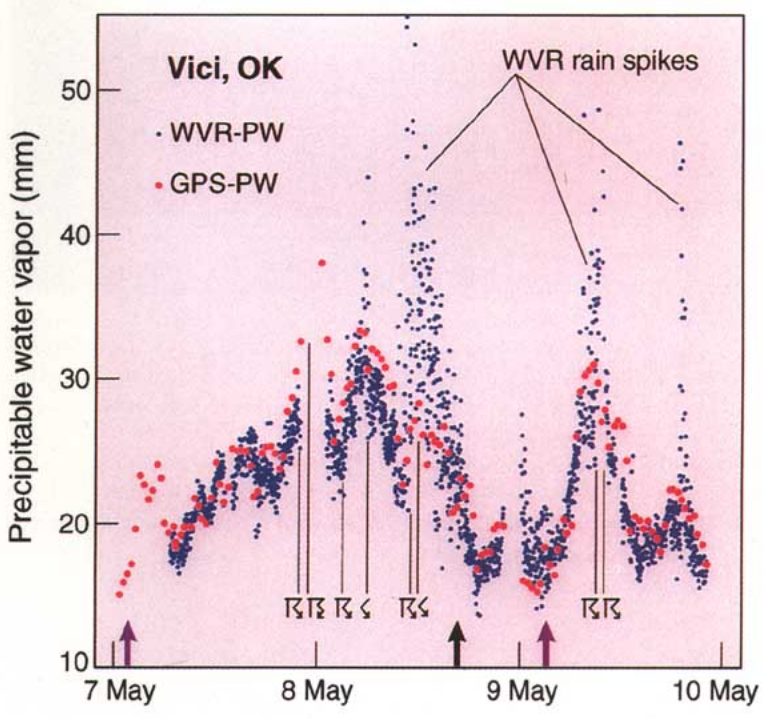

FIG. 5. Precipitable water at Vici for 1200 UTC 6 May to 0000 UTC 10 May 1994. The small blue dots represent radiometer measurements along the line of sight to GPS satellites, mapped to the zenith. The red dots represent 30-min averages of PW calculated from the least squares fits of GPS wet delay. Vertical arrows denote the time of the observed surface dryline passages at Vici. Time of thunderstorm activity is indicated with conventional symbols.

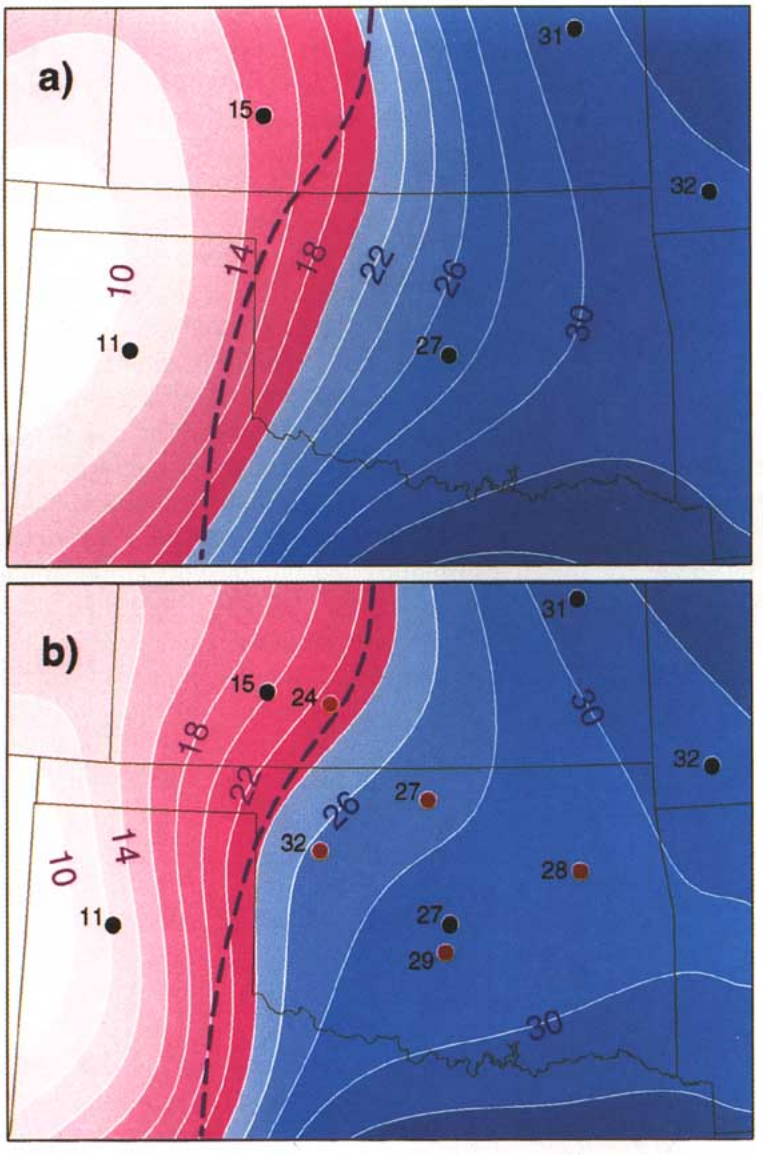

FIG. 6. (a) Objective analysis of precipitable water (in mm) using radiosonde derived PW data for 0000 UTC 8 May 1993. Small numbers indicate PW values at radiosonde sites (black circles). Purple dashed line in each panel indicates position of dryline analyzed by the National Meteorological Center. (b) Objective analysis of PW using radiosonde and GPS-derived PW data. Small numbers indicate PW values at radiosonde (black dots) and GPS sites (red dots) (adapted from Chiswell et al. 1996). The high PW value of 32 mm at Vici is consistent with thunderstorm activity observed in that area.

reveal more detail of the time evolution of the CFA than is available from NWP model output, satellite imagery, or radiosonde data alone. Water vapor density profiles can be obtained directly from radiosonde profiles (Fig. 8a) to obtain a time history of the evolution of the water vapor above a site.

The region of dry advection centered at ~600 mb can be distinguished from the more slowly changing boundary-layer moisture (<850 mb) in the radiosonde data (Fig. 8a). Using the relationship between PW and vapor density (ρ_v)

$$\mathrm{PW} = \rho_w^{-1} \int \rho_v dz, \qquad (5)$$

where ρ_w is the density of liquid water, and also using radiosonde profiles of ρ_v, the GPS-measured PW can be used to constrain the analysis of ρ_v in the period between radiosonde releases. By requiring the integrated vapor density at each time in the analysis to agree with the value obtained from the GPS, while maintaining the boundary conditions imposed by the sounding data, the resulting analysis more accurately reflects the temporal evolution of the vapor density profile between sounding times (Fig. 8b). The result of this method shows the CFA base near 800 mb, with a considerably sharper gradient in vapor density than is available from sounding data alone or that which can be resolved over the relatively coarse grid of the National Meteorological Center's Nested Grid Model. The location of the enhanced gradient coincides in time with the onset of thunderstorms activity at Purcell and at Norman, Oklahoma.

The above case study examples from GPS/STORM are for illustrative purposes. Ongoing research will be required to more fully evaluate the utility of the Earth-based GPS PW data in weather analysis and forecasting as additional data from this method become available and are combined with other operational data sources and assimilated into NWP models. The reader is referred to Chiswell et al. (1996) for a more complete description of the weather conditions surrounding the dryline, CFA cases reviewed here, and the application of GPS PW data in weather analysis.

In comparing the PW data from GPS and radiometers taken during GPS/STORM, an rms agreement of 1.0 to 1.5 mm is found (Duan et al. 1996). It is noteworthy that GPS measurements outperform those of the radiometers during periods of rain. Under these

conditions, the radiometer data are significantly degraded by the presence of water droplets on the microwave windows of the Radiometrics microwave radiometers deployed in the field experiment. The presence of rain, drizzle, or dew causes erroneously high and variable reports of PW, as seen in Figs. 5 and 7. This difficulty is a drawback in using the radiometer as a reference with which to lever a network of GPS receivers. By contrast, the absolute estimation technique, which relies only on GPS data, is not affected by precipitation.

4. Discussion

The meteorological applications of GPS fall into two classes—those that require observations in near real time, such as numerical weather prediction, and those, such as climate studies, in which the delay between data collection and data processing is not an important issue. Climate studies make no demands related to timing but benefit from data that have been processed with the most precise orbits available (currently <0.5 m absolute error). The quality of the orbits improves as the number of tracking sites used to calculate the orbits increases. A benefit of the addition of a space-based receiver in the geometry of the Earth-based tracking network is the prospect of improved GPS orbits.

To be of greatest value to the operational forecasting community, data from Earth-based GPS networks and LEO receivers must be collected in a central location and processed with accurate GPS orbits, in near real time (within the hour).[3] High quality orbits (~0.5 m absolute error) are available from the International GPS Service 7 to 10 days after data collection. Since these orbits are used almost exclusively for postprocessing of survey and scientific data, this delay has not presented a problem. As the demand for real-time data for weather (and earthquake) prediction has risen, increased attention has been focused on the development of near-real-time orbits. Two possible approaches are to compute GPS orbit corrections simultaneously with PW estimates or to make short-term (~1 day) orbit predictions. The Scripps Orbit and Permanent Array Center has recently initiated a rapid orbit determination using orbit predictions. SOPAC-predicted orbits have recently achieved an accuracy approaching that of the postprocessed orbits used in calculating the GPS/STORM PW data shown in this paper (Y. Bock 1995, personal communication).

A number of research opportunities exist for optimizing the complementary nature of the methods of active atmospheric monitoring by GPS described here and other observation systems currently in use. A few promising examples will be mentioned here. The space- and Earth-based approaches to monitoring the Earth's atmosphere are complementary in a number of ways.

1) Most Earth-based measurements involve vertical integration or averaging of atmospheric properties, whereas the space-based approach involves significant lateral averaging. Earth-based networks will be able to estimate lateral gradients in integrated water vapor at each station, whereas a single occultation event provides no significant information on lateral variability.

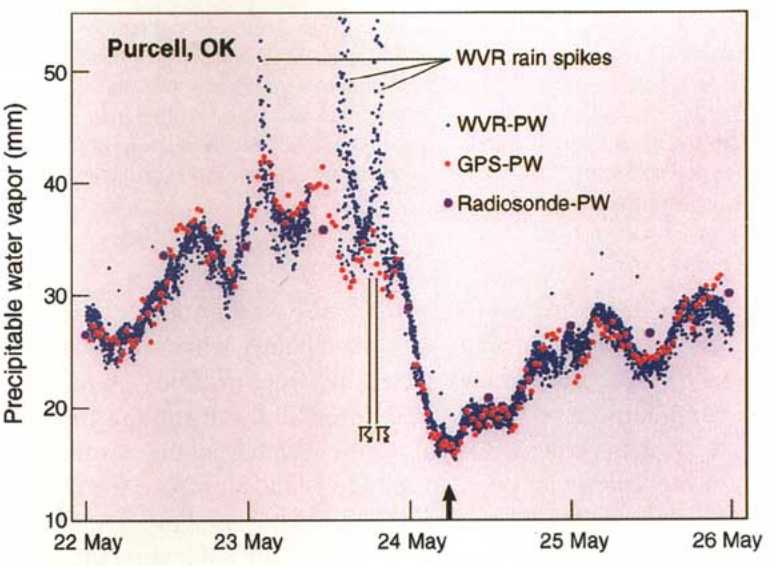

FIG. 7. Precipitable water at Purcell as measured by GPS, radiometer, and radiosonde from 0000 UTC 22 May to 0000 UTC 26 May 1993. The small blue dots represent radiometer measurements along the line-of-sight to GPS satellites, mapped to the zenith. The red dots represent 30-min averages of water PW calculated from the least squares fits of GPS wet delay. Twelve-hourly radiosonde data from Norman are shown by the purple dots. The vertical arrow denotes the time of the observed surface cold front passage at Purcell. Time of thunderstorm activity is indicated with conventional symbols.

[3]For perspective, the processing time for GPS PW data can be compared with the time it takes (~2 h) for a radiosonde to ascend.

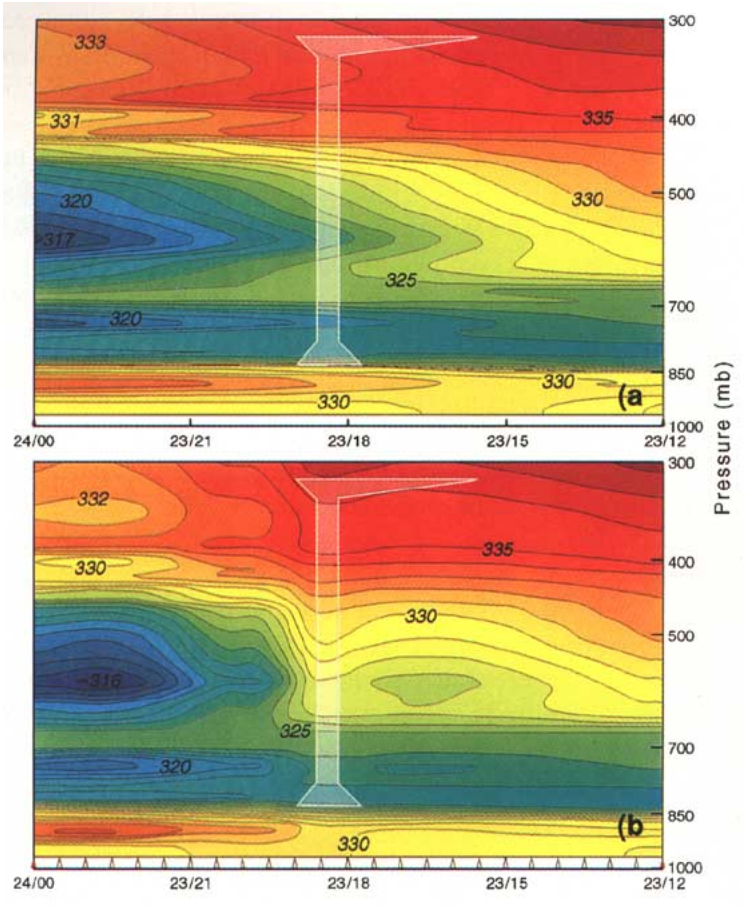

FIG. 8. (a) Time series cross section of equivalent potential temperature for 1200 UTC 23 May to 0000 UTC 24 May 1993 at Norman from radiosonde measurements. (b) Time series cross section of equivalent potential temperature with addition of GPS data constraints from Purcell. Cloud outline indicates time of thunderstorm activity. Small triangles along the bottom of the figure indicate times that GPS data are available. Labels along ordinate indicate date/UTC time (adapted from Chiswell et al. 1996).

2) Earth-based meteorology provides continuous measurements at a network of fixed points, whereas the space-based approach is discrete in time. Continuity in both space and time will be advantageous in contexts such as severe weather monitoring near major population centers and airports.
3) Because of the subhorizontal nature of its sampling geometry, space-based measurements are subject to obstruction by mountain ranges, and in adjacent low-lying areas, this may render much of the lower troposphere invisible.
4) Earth-based meteorology will never achieve good coverage over the oceans, whereas the space-based approach is essentially global. A GPS receiver in low Earth orbit with an inclination of at least 65° will provide refractivity profiles from approximately 500 GPS occultations per day distributed over the globe.

The relatively good vertical resolution and poor horizontal resolution of the GPS profiles are similarly complementary to those of nadir radiometric soundings. Preliminary results show that LEO-derived temperature soundings are comparable to radiosonde soundings in resolving the tropopause inversion (Ware et al. 1996). Knowledge of the spatial character of the tropopause has application in diagnosing potential vorticity anomalies and tropopause folds, which play a pivotal role in cyclogenesis (e.g., Hoskins et al. 1985). Over ocean areas, satellite radiometric radiances from operational polar and geostationary satellites are employed to construct soundings (Hayden 1988). Like soundings derived from Earth-based GPS receivers, radiometric soundings have high horizontal resolution and poor vertical resolution (~3 km). Since the measurement errors for these Earth- and space-based systems are largely independent, the estimation of atmospheric profiles of water vapor and temperature by a combined approach that includes data from Earth- and space-based GPS techniques and from satellite radiometer will be more accurate and provide better coverage than could be achieved by these methods alone (Suomi 1993).

The Earth- and space-based GPS techniques may be able to play a role in the development of a combined remote sensing capability that could eventually replace or reduce reliance on radiosondes. Integrated water vapor derived from Earth-based receivers can be distributed vertically according to ancillary information such as radiosonde or NWP model data (Chiswell et al. 1996). However, given a dense array of Earth-based receivers, the set of vectors from each receiver to each GPS satellite over a finite period of time represents a dense sampling of the troposphere above the array and could be processed using a technique similar to CAT scan tomography to provide information on the vertical distribution of water vapor. The vertical resolution provided by such an array

would depend upon the number of receiving antennas and their spatial distribution and is the subject of future research. There is potential for Earth-based GPS measurements to complement ground-based radio acoustic sounding system (RASS) measurements (Matuura et al. 1986), which provide information on the virtual temperature profile. The installation of GPS receivers at profiler sites in the Midwest, where RASS is also being tested, allows this potential to be investigated further (NOAA 1995). The opportunity for synergy between WSR-88D radar data and humidity data derived from GPS should also be mentioned.

The NWS is increasingly employing powerful workstations for data assimilation and graphical display to facilitate the analysis of new data streams from WSR-88D radars, the automated surface observing system, and satellites and to construct mesoscale forecasts for timely dissemination. In this context, GPS data can be incorporated in data assimilation systems for integration in mesoscale NWP models (Benjamin et al. 1991). Since the Earth-based GPS data represent the total integrated water vapor in the column, they provide a powerful constraint for NWP models. Mesoscale numerical model simulations have shown that when model-predicted precipitable water is relaxed toward an observed value, the model recovers the vertical structure of water vapor with an accuracy much greater than that found in statistical retrieval based on climatology, leading to improved short-range precipitation forecasts (Kuo et al. 1993). Data on the direction and magnitude of horizontal gradients in PW present an additional model constraint. Finally, data resolution over ocean areas in global NWP models should improve when refractivity profiles from space-based receivers are directly ingested. Studies with simulated space-based GPS profile data conclude that the optimum way of using the data in numerical weather prediction models may be to assimilate vertical profiles of atmospheric refractivity directly into the model (Eyre 1994; Zou et al. 1995), rather than separating temperature and humidity data first.

Concerns that arise in the context of GPS technology and real-time estimation are the effects of selective availability (SA) and antispoofing. The Department of Defense implemented SA in March 1990 in order to deny most civilian users of the system the maximum achievable accuracy in navigation applications by corrupting the signal structure. Although this policy has affected many civilian users of GPS, it has not had a significant impact on geodetic (relative positioning) applications (e.g., Rocken and Meertens 1991). Provided that all receivers sample the GPS signal close to simultaneously, the effect of SA can be eliminated after the fact. Consequently, SA is not a significant problem for GPS meteorology. However, it does affect the efficiency with which GPS processing applications can provide real-time estimates of PW for operational applications. Antispoofing is meant to stop false signals from misleading military receivers by encrypting the codes superimposed on both microwave carrier waves transmitted by the GPS satellite. New receiver architectures have addressed this issue.

The prospect of using Earth-based GPS data to measure atmospheric water vapor for research and operational weather forecasting is promising because extensive networks of continuously operating Earth-based GPS receivers are now being installed around the world by geophysicists, geodesists, surveyors, and others for a variety of scientific, engineering, and civilian navigation and positioning applications (Table 1, Fig. 9). GPS-derived PW data could be made available to the research and operational meteorological community at relatively little incremental cost.

Several hundred new private (communication) and government satellites have been announced for launching in the next several years (Ware 1992).[4]

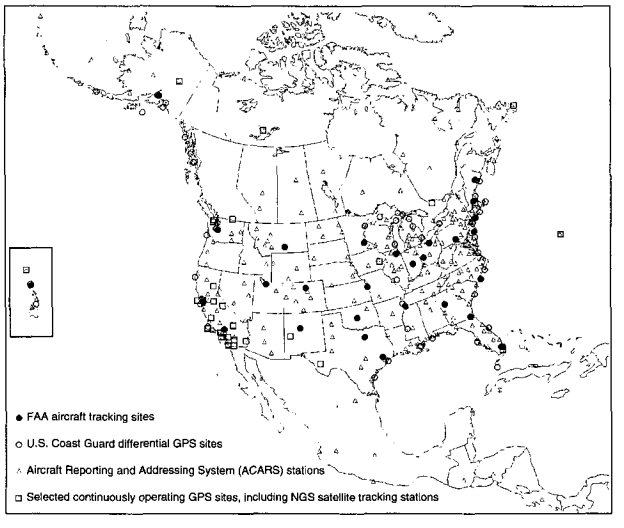

FIG. 9. Location of proposed Aircraft Reporting and Addressing System differential GPS Stations (triangles), proposed FAA aircraft tracking sites (•), selected continuously operating GPS sites including NGS satellite tracking stations (squares), and U.S. Coast Guard differential GPS sites (open circles).

[4]Satellites such as *TOPEX/POSEIDON, Gravity Probe-B, ARISTOTELES,* and *EOS-B* are carrying, or plan to carry, GPS receivers.

TABLE 1. Continuously operating Earth-based GPS receivers by network. Current GPS receivers are those already installed; proposed are those planned for installation in the near future (after Ware and Businger 1995).

Location	Current	Proposed	Sponsor
Antarctica	3	3	Australian and German governments/National Aeronautic and Space Administration (NASA)
Australia		7	Australian government
Canada	4	2	NASA
Canadian coastal stations		25	Canadian Coast Guard
Fennoscandia	16	8	Finnish, Norwegian, and Swedish governments
Japan		290	Japanese government
Mississippi Basin		15	U.S. Army Corps of Engineers
California	46	268	NASA/National Science Foundation (NSF)/U.S. Geological Survey (USGS)
Philippines		3	Australian and Japanese governments
U.S. airports	5	300	Federal Aviation Administration
U.S. coastal stations	6	50	U.S. Coast Guard
U.S. Midwest	4	28	NOAA
U.S. states	20	80	NGS/state governments
U.S. (other)		251	National Geodetic Survey (NGS)/NSF/USGS
Worldwide (other)	71	114	Defense Mapping Agency (DMA)/ NASA/NSF/NGS/Other governments
Subtotals	**175**	**1444**	
Total current and proposed	**1619**		

Many of these satellites will carry GPS receivers for tracking and attitude measurements. With the demonstrated early promise of the GPS occultation technique for providing useful atmospheric data, the potential for gaining additional refractivity, temperature, and humidity data from this method is considerable. Due to their global coverage, these data may provide the best opportunity to date for monitoring the global climate by observing changes in mean refractivity profiles (Yuan et al. 1993).

5. Conclusions

Measurement of atmospheric water vapor by Earth-based GPS receivers was demonstrated during the GPS/STORM field project to be comparable, and in some respects superior, to that by ground-based water vapor radiometers. Increased spatial and temporal resolution of the water vapor distribution from the GPS/STORM network proved valuable in monitoring the moisture flux convergence associated with thunderstorm development associated with an evolving dryline and the decrease in integrated water vapor associated with the passage of a midtropospheric cold front, both of which triggered severe weather over the area during the course of the experiment.

The first space-based GPS receiver designed for sensing the Earth's atmosphere was launched in April 1995. Preliminary results of this approach indicate that temperature profiles obtained from the refractivity data in the mid- to upper troposphere and lower stratosphere (Ware et al. 1996) can identify sharp temperature inversions characteristic of the tropopause with a resolution approaching that of radiosonde soundings. In principle, humidity profiles can be obtained from the refractivity profiles wherever the temperature distribution is known from other sources, such as radiosondes, or over tropical regions where horizontal and temporal variations in the temperature are small and

reasonably well represented in global weather prediction models.

In conjunction with operationally available datasets, PW data from Earth-based receivers and refractivity profiles from space-based receivers represent a potentially important new resource for operational numerical weather prediction. The development of models that produce accurate orbit predictions is a step toward realizing this potential. Archived datasets from GPS networks and space-based receivers could prove valuable in basic research of mesoscale and synoptic-scale weather systems, the hydrologic cycle, and global climate change.

Although GPS measurements of the atmosphere have the potential to enhance the analysis and prediction of weather and climate, significant research is required to assess this potential in detail and to develop capabilities to derive maximum benefit from these new sources of atmospheric data. Further research is needed to determine how these data can most effectively be processed in combination with other data resources and assimilated into weather prediction models.

Acknowledgments. We would like to thank Seth Gutman (NOAA/FSL) and Ted Cress (Battelle NW) for their support of the GPS/STORM project. This research was supported by the National Science Foundation under Grants ATM-9207111, ATM-9496335, EAR-911756, and EAR-9116461. UNAVCO provided facilities and equipment under NSF Grant EAR-9116461. NCAR and NOAA/Environmental Testing Laboratory provided surface meteorological and additional radiometer data. Radiometrics Inc., Boulder, Colorado, loaned water vapor radiometers, and Paroscientific loaned a precise barometer for use in GPS/STORM.

References

Askne, J., and H. Nordius, 1987: Estimation of tropospheric delay for microwaves from surface weather data. *Radio Sci.*, **22,** 379–386.

Barat, J., and C. Cot, 1995: Accuracy analysis of Rubsonde-GPS tracking wind sounding system. *J. Appl. Meteor.*, **34,** 1123–1132.

Benjamin, S. G., and K. A. Brewster, R. Brummer, B. F. Jewett, T. W. Schlatter, T. L. Smith, and P. A. Stamus, 1991: An isentropic three hourly data assimilation system using ACARS aircraft observations. *Mon. Wea. Rev.*, **119,** 888–906.

Bevis, M., S. Businger, T. A. Herring, C. Rocken, R. A. Anthes, and R. H. Ware, 1992: GPS Meteorology: Remote sensing of atmospheric water vapor using the Global Positioning System. *J. Geophys. Res.*, **97,** 15 787–15 801.

——, ——, ——, R. A. Anthes, C. Rocken, R. H. Ware, and S. R. Chiswell, 1994: GPS Meteorology: Mapping zenith wet delays onto precipitable water. *J. Appl. Meteor.*, **33,** 379–386.

Boire, G., E. C. Souter, and S. P. Pryor, 1993: A low cost GPS rawinsonde system. Preprints, *Eighth Symp. on Meteorological Observations and Instrumentation,* Anaheim, CA, Amer. Meteor. Soc., 23–24.

Brunner, F. K., and M. Gu, 1991: An improved model for the dual frequency ionospheric correction of GPS observations. *Manuscr. Geod.*, **16,** 205–214.

Businger, S., W. H. Bauman III, and G. F. Watson, 1991: Coastal frontogenesis and associated severe weather on 13 March 1986. *Mon. Wea. Rev.*, **119,** 2224–2251.

——, S. R. Chiswell, W. C. Ulmer, and R. Johnson, 1996: Balloons as a Lagrangian measurement platform for atmospheric research. *J. Geophys. Res.*, in press.

Charba, J. P., 1979: Two to six hour severe local storm probabilities: An operational forecasting system. *Mon. Wea. Rev.*, **107,** 268–282.

Chiswell, S. R., S. Businger, M. Bevis, C. Rocken, R. Ware, T. VanHove, and F. Solheim, 1996: Application of GPS water vapor data in severe weather analysis. *Mon. Wea. Rev.*, submitted.

Davis, J. L., T. A. Herring, I. I. Shapiro, A. E. Rogers, and G. Elgered, 1985: Geodesy by radio interferometry: Effects of atmospheric modeling errors on estimates of baseline length. *Radio Sci.*, **20,** 1593–1607.

Duan, J., and Coauthors, 1996: GPS meteorology: Direct estimation of the absolute value of precipitable water. *J. Appl. Meteor.*, in press.

Elgered, G., J. L. Davis, T. A. Herring, and I. I. Shapiro, 1990: Geodesy by radio interferometry: Water vapor radiometry for estimation of the wet delay. *J. Geophys. Res.*, **96,** 6541–6555.

Eyre, J. R., 1994: Assimilation of radio occultation measurements into a numerical weather prediction system. ECMWF Tech. Memo. No. 199, 34 pp. [Available from ECMWF, Shinfield Park, Reading RG2 9AX, United Kingdom.]

Fjeldbo, G. A., J. Kliore, and V. R. Eshleman, 1971: The neutral atmosphere of Venus as studied with the Mariner V radio occultation experiments. *Astron. J.*, **76,** 123–140.

Gorbunov, M. E., and S. V. Sokolovskiy, 1993: Remote sensing of refractivity from space for global observations of atmospheric parameters. Max-Planck-Institut fur Meteorologie Report No. 119. [ISSN 0937-1060.]

Gurvich, A. S., and T. G. Krasil'nikova, 1990: Navigation satellites for radio sensing of the Earth's atmosphere. *Soviet J. Remote Sens.*, **7**(6), 1124–1131.

Hayden, C. M., 1988: GOES–VAS simultaneous temperature–moisture retrieval algorithm. *J. Appl. Meteor.*, **27,** 705–733.

Herring, T. A., 1992: Modeling atmospheric delays in the analysis of space geodetic data. *Proc. Symp. on Refraction of Transatmospheric Signals in Geodesy,* Delft, the Netherlands, Netherlands Geodetic Commission, 157–164.

Hobbs, P. V., J. D. Locatelli, and J. E. Martin, 1990: Cold fronts aloft and the forecasting of precipitation and severe weather east of the Rocky Mountains. *Wea. Forecasting,* **5,** 613–626.

Hoskins, B. J., M. E. McIntyre, and A. W. Robertson, 1985: On the use and significance of isentropic potential vorticity maps. *Quart. J. Roy. Meteor. Soc.*, **111,** 877–946.

IPCC, 1992: *Climate Change 1992.* J. T. Houghton, B. A.

Callander, and S. K. Varney, Eds., University of Cambridge Press, 200 pp.

Kuo, H. L., 1965: On the formation and intensification of tropical cyclones through latent heat release by cumulus convection. *J. Atmos. Sci.,* **22,** 40–63.

Kuo, Y.-H., Y.-R. Guo, and E. R. Westwater, 1993: Assimilation of precipitable water into a mesoscale numerical model. *Mon. Wea. Rev.,* **121,** 1215–1238.

——, X. Zou, and Y.-R. Guo, 1996: Variational assimilation of precipitable water using a nonhydrostatic mesoscale adjoint model, Part I: Moisture retrieval and sensitivity experiments. *Mon. Wea. Rev.,* in press.

Leick, A., 1990: *GPS Satellite Surveying.* John Wiley & Sons, 352 pp.

Lindal, G. F., and Coauthors, 1981: The atmosphere of Jupiter: An analysis of the voyager radio occultation measurements. *J. Geophys. Res.,* **86,** 8721–8727.

Locatelli, J. D., J. M. Sienkiewicz, and P. V. Hobbs, 1989: Organization and structure of clouds and precipitation on the mid-Atlantic coast of the United States. Part 1: Synoptic evolution of a frontal system from the Rockies to the Atlantic coast. *J. Atmos. Sci.,* **46,** 1327–1348.

Matuura, N., Y. Masua, H. Inuki, S. Kato, S. Fukao, T. Sato, and T. Tsuda, 1986: Radio acoustic measurement of temperature profiles in the troposphere and stratosphere. *Nature,* **323,** 426–428.

McCarthy, J., and S. E. Koch, 1982: The evolution of an Oklahoma dryline. Part I: Meso- and subsynoptic-scale analysis. *J. Atmos. Sci.,* **39,** 225–236.

Melbourne, W. G., 1976: Navigation between the planets. *Sci. Amer.,* **234,** 58–74.

——, and Coauthors, 1994: The application of spaceborne GPS to atmospheric limb sounding and global change monitoring. JPL Publication 94-18, 147 pp.

NOAA, 1995: Precipitable water vapor comparisons using various GPS processing techniques. Document No. 1203-GP-36, 35 pp. [Available from NOAA ERL FSL, Boulder, CO.]

Parsons, D. B., M. A. Shapiro, R. M. Hardesty, R. K. Zamora, and J. M. Intrieri, 1991: The finescale structure of a west Texas dryline. *Mon. Wea. Rev.,* **119,** 1242–1258.

Rocken, C., and C. Meertens, 1991: Monitoring selective availability dither frequencies and their effect on GPS data. *Bull. Geodesique,* **65,** 162–169.

——, R. Ware, T. VanHove, F. Solheim, C. Alber, J. Johnson, M. Bevis, and S. Businger, 1993: Sensing atmospheric water vapor with the Global Positioning System. *Geophys. Res. Lett.,* **20,** 2631–2634.

——, T. VanHove, J. Johnson, F. Solheim, R. H. Ware, M. Bevis, S. Businger, and S. R. Chiswell, 1995: GPS/STORM—GPS sensing of atmospheric water vapor for meteorology. *J. Atmos. Oceanic Technol.,* **12,** 468–478.

Saastamoinen, J., 1972: Atmospheric correction for the troposphere and stratosphere in radio ranging of satellites. *The Use of Artificial Satellites for Geodesy, Geophys. Monogr.,* Ser. 15, AGU, 247 pp.

Schaefer, J. T., 1974: The life cycle of the dryline. *J. Appl. Meteor.,* **13,** 444–449.

Spilker, J. J., 1980: Signal structure and performance characteristics. *Global Positioning System,* Vol. 1, The Institute of Navigation, 246.

Stephens, G. L., and T. J. Greenwald, 1991: The Earth's radiation budget and its relation to atmospheric hydrology. 1. Observations of the clear sky greenhouse effect. *J. Geophys. Res.,* **96,** 15 311–15 324.

Suomi, V. E., 1993: Final Report to Space System/Loral. [Available from Suomi Scientific, Inc., 10 Rosewood Circle, Madison, WI 53711.]

Waldstreicher, J. S., 1989: A guide to utilizing moisture flux convergence as a predictor of convection. *Natl. Wea. Dig.,* **14,** 20–35.

Ware, R., 1992: GPS sounding of Earth's atmosphere. *GPS World,* **3,** 56–57.

——, and S. Businger, 1995: Global positioning for geosciences research. *Eos, Trans. Amer. Geophys. Union,* **76,** 187.

——, C. Rocken, and K. Hurst, 1986: A GPS baseline determination including bias fixing and water vapor radiometer corrections. *J. Geophys. Res.,* **91,** 9183–9192.

——, and Coauthors, 1996: GPS sounding of the atmosphere from low Earth orbit: Preliminary results. *Bull. Amer. Meteor. Soc.* **77,** 19–40.

Yuan, L., R. Anthes, R. Ware, A. Rocken, W. Bonner, M. Bevis, and S. Businger, 1993: Sensing global climate change using the Global Positioning System. *J. Geophys. Res.,* **98,** 14 925–14 937.

Zou, X., Y.-H. Kuo, and Y.-R. Guo, 1995: Assimilation of atmospheric radio refractivity using a nonhydrostatic mesoscale model. *Mon. Wea. Rev.,* **123,** 2229–2249.

Zumberge, J., R. Neilan, and J. Kouba, 1994: The international GPS service for geodynamics—Benefits to users. Proc. Institute of Navigation, 7th Technical Meeting, Salt Lake City, UT, 1663–1666.